444Insights into the continuous staggered bioleaching of pure copper from waste printed circuit boards

Zahra Ilkhani[a], Joshua Redman[a], Evie Stokes[a], Ken Parker[b], Farid Aiouache[a*]

[a]Engineering department, Lancaster University, Bailrigg, Lancaster, LA1 4YW, UK

[b]ICT Reverse Asset Management ltd, 2 Mannin way, LA1 3SU, Lancaster, UK

[*]Corresponding author: f.aiouache@lancaster.ac.uk

Abstract

Recycling precious metals from electronic waste by bioleaching stands out as a sustainable technology for metal solubilisation using microorganisms. In this study, the recovery of pure copper from waste printed circuit boards was performed through an indirect approach by sequential bioleaching and electrowinning. The bacterium *Acidithiobacillus ferrooxidans* was cultivated in a stirred tank reactor for the continuous production of ferric iron (Fe^{3+}) as the primary leaching agent for batch leaching at pulp densities and temperature up to 8% w/v and 40 °C, respectively. A leaching rate of 50% copper was achieved at a pulp density of 6% w/v, 40 °C and 96 hours spent time. The finding was used as a reference for a flow leaching operations in a continuous stirred tank reactor and rates of 100% and 80% of copper were leached with and without pH control, respectively, at 40 °C and a hydraulic residence time of 96 hours. A rate of 70.85% of pure copper was then recovered from the metal rich solution by electrowinning using a current density of 0.0168 A/cm^2 over 8 hours. These results provide valuable insights into the continuous recovery of copper from electronic wastes and contribute to the ongoing strategies of design and scale-up toward industrially viable operations.

Keywords: Waste printed circuit board, Bioleaching, Continuous Stirred tank reactor, Electrowinning, Electronic waste, Acidophilic microorganism

1. Introduction

Nowadays, there has been rapid growth of electrical and electronic appliances which once spent are leading to a significant release in the production of electronic and electric waste (E-waste) at a rate of two to three times faster than other wastes (Priya and Hait, 2017; Vardanyan et al., 2022b). In 2019, the value of raw materials in e-waste was estimated at approximately USD 57 billion, with printed circuit boards (PCBs) being the most valuable component of e-waste (Van Yken et al., 2023). PCBs have varied compositions but consist mainly of a 28% metallic portion made of Cu, Al, Ni, Co, Au, and Ag, and a 72% non-metallic portion of plastics and ceramics (Priya and Hait, 2017). The PCBs contain around 20-30% copper, which is appreciated for its affordable conductivity, and 3500 ppm of precious metals such as Au (20-250 ppm), Ag (200-3000 ppm) and Pt (10-200 ppm), which makes them a promising secondary source for valuable metal recycling (Trivedi and Hait, 2023).

The recycling technology of metals continues adopting mature techniques based on pyrometallurgy and hydrometallurgy, operating at high temperatures and in the presence of acid/alkali-based solutions, respectively (Ilkhani et al., 2024). These methods require high investment (i.e. 8000 $/ton), consume high energy (i.e. 30 MJ/ton) and produce secondary pollution (i.e. 2270 kg/ton) (Arya and Kumar, 2020; Xu et al., 2021), drawing attention to develop environmentally friendly and cost-effective alternative such as the bioleaching which uses a judicious combination of biotechnology and the hydrometallurgy in the presence of biocatalyst-based microorganisms for the selective production of essential leaching agents (Sadeghi et al., 2024; Xia et al., 2017). *Acidithiobacillus ferrooxidans* (*A. ferrooxidans*) has been the most studied bacterium in the bioleaching of Cu from waste PCBs due to its high tolerance to heavy metals and acidic conditions, and resistance to contamination by unwanted substrates (Arshadi et al., 2021). In acidophilic bioleaching by *A. ferrooxidans*, ferrous iron

(Fe^{2+}) is the main energy source, which is oxidised to ferric iron (Fe^{3+}) Eq. (1), an oxidising agent that solubilises metals such as Cu into Cu^{2+} (Eq. (2) (Pathak et al., 2014; Rodrigues et al., 2015). An interesting example is the work by Bryan et al., (2015) who reported the bioleaching rates of 100% Cu, 92% Ni, and 89% Zn from waste PCBs using *A. ferrooxidans.* Arshadi and Yaghmaei, (2020) reported leaching rates of Cu (90%) and Ni (88%) from PCBs by *A. ferrooxidans* at a pulp density of 1.5% (w/v) with pH control.

$$4Fe^{2+} + 4H^{+} + O_2 \rightarrow 4Fe^{3+} + 2H_2O \quad (1)$$

$$2Fe^{3+} + Cu \rightarrow Cu^{2+} + 2Fe^{2+} \quad (2)$$

Most works reported in open literature have been carried out using one step method where the addition of e-waste and bacteria to the media takes place at the same time, affecting inevitably the activity of the microorganisms in direct contact with the e-waste. In the two-step method, the bacteria are grown in a separate medium until they reach the logarithmic growth phase and then the e-waste is added to the medium. Unlike in the one-step method, the bacteria and waste in the spent medium are not in direct contact in two-step method, enabling flexible degrees of freedom of the thermodynamic limitations to be adapted to the operating conditions of mass, heat and momentum transports, accessible through the pulp density, temperature and mixing, respectively, without the bacterial load limitation (Dong et al., 2023). Noting the barrier of toxicity by the metallic and non-metallic components of the microorganisms (i.e. oxygen availability, shear stress of the flow dynamics and mass transfer limitations) which slows down the dissolution of metal ions and the bacterial growth, most studies reported the bioleaching of PCBs at low pulp density (Guo et al., 2023; Van Yken et al., 2023). Yang et al., (2014) for instance reported high bioleaching rates of Cu (96.8%), Zn (83.8%), and Al (75.4%) at a pulp density of 1.5% (w/v) by *A. ferrooxidans* but noticed inhibition of the microbial growth at high pulp densities. Xin et al., (2012) demonstrated a complete deactivation of iron-oxidizing bacteria at a pulp density of 2 %, while 100% Zn was leached at a pulp density of 1%. Tapia et al., (2022) observed bacterial growth of a mixed culture containing *Tissierella*, *Acidophilium*, and *Leptospirillum* at 0.5% PCBs, limited growth at 1.5% PCBs and no growth at 2% PCBs during the bioleaching of heavy metals from waste PCBs. Pradhan and Kumar, (2012) found that the consortium of *C. violaceum*, *P. aeruginosa*, and *P. fluorescens* was able to leach 69.3% Au from waste PCBs at a pulp density of 1%, but the leaching rate decreased to 20.28% when the pulp density was increased to 10%.

Other option by bacteria adaptation to toxic metals remains a time-consuming process due to the complex control of process parameters and various PCB nature and composition (Vardanyan et al., 2022a). In one study, Arshadi et al., (2021) investigated the bioleaching of base metals from PCBs using adapted *A. ferrooxidans* in the bubble column bioreactor. The adaptation process involved a gradual increase of the waste concentration from 1 to 15 g/L in a flask for 187 days, then an additional increase to 40 g/L in bubble column bioreactors for 44 days, resulting in 54% of Cu, 75% of Ni and 55% of Fe recovery under the optimum condition of 20 g/L of solid content after 9 days. In another study, Tapia et al., (2022) utilised a consortium of mesophilic bacteria adapted to PCBs waste through the serial acclimation method. After 2 days of growth, PCB waste was added at an initial concentration of 2.5 g/L for 4 days which was then increased to 5 g/L and resulted in a leaching rate of 69% Cu and 91% Zn over 18 days.

Despite the advancement observed in PCB bioleaching with high metal extraction, to the authors' knowledge no commercial bioleaching for PCBs has been developed yet which could be justified partly by the inhibition of microbial cultures by the metals, especially when aiming to use high pulp densities to reach an economically viable design. The non-contact leaching in the two-step method has been however recurrently cited as the promising approach that allows the use of high pulp densities and opens possibilities for sustainable development of industrial scale operations at reduced constraints in comparison with the one-step direct contact process (Adam et al., 2024; Hubau et al., 2020). For example, in a non-contact leaching by biogenic lixiviant produced by *A. ferrooxidans* and *A. thiooxidans,* 53.2% Co, 60.0% Li, 48.7% Ni, 81.8% Mn and 74.4% Cu were extracted from the lithium-ion battery at 10% (w/v) pulp density (Boxall et al., 2018). Hosseini Nasab et al., (2021) reported leaching rates of Ni (83.65%), Co (86.93%) and Fe (64.34%) by the supernatants from *A. ferrooxidans* from an iron-rich laterite ore with a pulp density of 10%. Wu et al., (2018) achieved 93% Cu extraction from 10% (w/v) PCB solids loaded over a period of 9 days using a two-stage process while the leaching agent (15 g/L Fe^{3+}) was produced in a batch culture of *L. ferriphilum* and *Sulfobacillus thermosulfidooxidans*.

Scaling up the laboratory tests has been an important challenge in bioprocessing in order to achieve enhancement in the readiness level from both microbiological and technological perspectives and bring them as close as possible to industrial applications. On a laboratory scale, shake flasks are commonly used but the stirred tank reactors (STR) are the bioreactors in essence for the scaleups because of the improved control of the design parameters such as pH, temperature, agitation and aeration of the medium (Arshadi et al., 2021; Mahmoud et al., 2017; Tapia et al., 2022). Compared to the batch reactor, the continuous stirred-tank reactor (CSTR) is one of the engineered reactors that enables more efficient control of capital and operating costs along with an integrated supply of the energy and nutrient sources for the bacterial growth, even under non-sterile conditions (Chen et al., 2022). Recently, Hubau et al., (2020) employed an acidophilic consortium for the bioleaching of metals in a CSTR and demonstrated a leaching rate of 96% Cu, 73% Ni, 93% Co and 85% Zn at 1% PCB and hydraulic residence time (HRT) of 48 h. Cancho et al., (2007) used moderate thermophilic microorganisms and silver ions as an enhancer in a series of 3 CSTRs to leach approximately 66% Cu at 45 °C, 2 g silver per kilogram of a chalcopyrite concentrate. The residence time was increased from 7 to 14 days, as the duration was insufficient for the solubilisation at the designed scale. Chen et al., (2022) reported a leaching efficiency of Zn (78%), Ni (90%), Cu (90%) and Cr (68%) from contaminated sediment using several acidophilic sulphur-oxidizing bacteria at HRT of 10 days with a sulphur dosage of 5%. An increase in the sulphur dosage was demonstrated to enhance the pH reduction, sulphate production, and metal leaching rates due to the higher substrate availability for sulphur-oxidizing bacteria.

The purification methods based on ion exchange, cementation, sulphide precipitation and electrowinning continue to be adopted at industrial scale production of pure Cu produced by the conventional chemical leaching process (Fathima et al., 2022). The electrowinning process of Cu in the context of the composition of leachates released by the PCBs is seen as a cost-effective method facilitated by the thermodynamic chemical potentials of the associated leached metals and no requirements of additional reagents (Pakostova and Herath, 2023). Only a few studies however have been reported on electrowinning coupled with bioleaching. Baniasadi et al., (2021) investigated the recovery of 75.8% of Cu after bioleaching by *A. ferrooxidans* and noted a promising selectivity promoted by the reduced interference of other metals available in PCBs. This observation was confirmed by (Pakostova and Herath, 2023), who demonstrated a recovery of 99% pure Cu after a 3.33 h operation.

In the present study, the two-step indirect approach is performed to recover pure metallic Cu from waste PCBs of high pulp density under continuous flow operations. The first stage is dedicated to the production in a CSTR of biogenic Fe^{3+} ions which are used as a source for continuous leaching in the second stage. Most previous studies have focused on using ferrous-oxidizing bacteria within a single reactor for both Fe^{3+} production and PCB leaching (Becci et al., 2021; Işıldar et al., 2016), while this study aims to investigate the efficiency of the process when the bioreactor for Fe^{3+} generation is separated from the leaching reactor to validate the reduction in the boundary limitation of the single step process at high pulp density, paving the way for a strategy towards the process scaleup. Effects of the key operating parameters such as temperature, pH and hydraulic residence time on the leaching efficiency are examined and the associated chemical mechanism is discussed. Fig. 1. illustrates the schematic diagram of the whole process in this study. To the best of our knowledge, there have been no studies regarding the use of indirect continuous bioleaching for Cu extraction from waste PCBs with a high pulp density.

2. Methods and materials

2.1. Pre-processing of PCBs

The waste computer PCBs were provided by ICT Reverse©. All the main parts of electronic components (i.e. capacitors, plastics, batteries, and resistors) were dismantled manually by a screwdriver and cut into small pieces (5cm × 5cm) by a metal guillotine cutter. The PCB samples were dipped overnight in a 5M NaOH to remove the coating, as the solder mask was observed not to facilitate the leaching agent to penetrate the surface of solid waste and solubilise metals easily. Further size reduction was run using a blender. Finally, the PCBs were sieved through a mesh number 200 to reach a powder with a particle size of approximately ~78 µm. To determine metal concentrations, 0.1g of the PCB sample was added to the microwave vessel (CEM Discover SP-D, CEM Corporation, United States) and treated with Aqua Regia (15 mL; prepared from HNO_3:HCl (1:3 v/v, HNO_3 70%, HCl 35%). The metal content of the mixture was measured directly by Inductively Coupled Plasma Optical Emission Spectroscopy (ICP-OES) (Agilent 5100 VDV, Agilent Technologies Inc, Australia). The Cu was identified as illustrated in Table 1 as the major metal in the powder.

2.2. Bacterial culture condition

Acidithiobacillus ferrooxidans (*A. ferrooxidans*) was grown in a shake flask as a batch culture in 9k media containing 3 g $(NH_4)_2SO_4$, 0.5 g K_2HPO_4, 0.5 g $MgSO_4.7H_2O$, 0.1 g KCl, 0.01 g $Ca(NO_3)_2$ and 44.22 g $FeSO_4.7H_2O$ in 1L deionized (DI) water. The pH was adjusted to 1.8 using H_2SO_4 (98%). The bacteria were put in a shaker incubator at 30 °C and a rotation speed of 140 rpm as an optimum growing condition for a week until the colour changed from green to red owing to the oxidation of Fe^{2+} to Fe^{3+} (Arshadi and Yaghmaei, 2020). Once the bacteria reached the logarithmic phase with a cell density of (2×10^7), the culture was transferred to a 2 L stirred tank reactor (STR). A continuous culture experiment was performed in a Continuous Stirred Tank Reactor (CSTR) (Armfield Ltd, CEM MKII) coupled with a circulating bath to maintain a constant operating temperature for the bacterial growth. Initially, the batch reactor was filled with 1 L fresh 9k media with a pH adjusted at 1.7-1.8. 10% v/v bacteria were inoculated and cultivated at 30 °C, and 140 rpm agitation speed, while the air was provided at 1-2 L/min air flow by Interpet™ air pump to maintain sufficient oxygen level for bacterial growth for 96 h as a start-up time until the bacteria grow (cell density~2.5×10^7 cells/ml). Then, the bacteria were fed continuously with a fresh media to the bottom of the reactor by a Longer™ YZ1515X peristaltic pump at a flow rate of 250 ml/d and the effluent containing biogenic Fe^{3+} and bacteria was continuously pumped out at HRT of 96 h. The pH was monitored daily and maintained at 1.8-1.9. After filtration through a 0.2 µm Corning® bottle-top vacuum filter, the biogenic Fe^{3+} was collected in a storage tank for further leaching.

2.3. Batch leaching of Cu

The indirect bioleaching experiments in a batch mode were carried out in an Erlenmayer flask using biogenic Fe^{3+} generated from the microbial culture of *A. ferrooxidans*. The effect of different pulp densities of powder (1%, 2%, 4%, 6% and 8%) was investigated at 40 °C and agitation speed of 200 rpm for 96 h and the concentration of Cu in the metal leach solution was measured using ICP-OES analysis.

2.4. Continuous leaching in a Stirred tank reactor (STR)

The indirect bioleaching experiments of the PCBs were performed in a 2 L glass stirred tank reactor containing baffles and an electric motor-driven paddle stirring at 300 rpm. The temperature within the reactor was maintained at a constant level using a water bath with circulating water. The biogenic Fe^{3+} and PCB powder were introduced into the reactor continuously by a Longer^{TM} YZ1515X peristaltic pump at a specific rate. The CSTR was operated under various conditions: at room temperature and 40 °C, with residence time of 48 and 96 h and pH control. pH and redox potential (Eh) were monitored daily and the concentration of Cu in the metal leach solution was investigated using ICP-OES analysis. All conditions were tested in duplicate.

2.5. Recovery of pure Cu by electrowinning

A 500 ml solution of leachate in a glass beaker, using a carbon electrode as anode and a stainless-steel sheet as cathode was prepared. A plating tape was used to cover the reverse side of the cathode surface to avoid Cu deposition. An area of 29.75 cm^2 of cathode was immersed in the solution of leachate stirred at 500 rpm using a magnetic stirrer to facilitate the mass transport of Cu ions to the cathode surface and operated for 8 h with a current density of 0.0168 A/cm^2 at room temperature. The mass of the deposited Cu was calculated by measuring the weight of cathode every hour.

2.6. Analytical methods

The concentration of Fe^{3+} was determined by the production of a calibration curve using the 5-sulfosalicyclic acid method and the absorbance of the solution was measured by Ultraviolet-Visible Spectroscopy (UV-VIS) (Evolution 220, Thermo Fisher Scientific, USA) at a wavelength of 500 nm. The total Fe concentration was determined by adding 0.3 ml of 25% ammonium hydroxide solution to the above solution and measuring the absorbance of the solution at 425 nm (Karamanev et al., 2002). The pH value was measured by pH meter (Accumet AE150, Fisher Scientific, USA) and the redox potential was measured using a platinum electrode with an Ag/AgCl reference electrode (Hl-2211, Hanna Instruments, USA). The surface morphology of the powder before and after bioleaching was observed via field emission scanning electron microscopy (FE-SEM) equipped with Energy-dispersive X-ray spectroscopy (EDX) (JSM-7800F, JEOL Ltd, Japan). The component phases and the structure of powder before and after bioleaching were determined using X-ray diffraction (XRD) (SuperNova, Agilent Technologies, USA).

3. Results and discussions

3.1. Bacterial cultivation in a reactor

The bacterial behaviour and the production of Fe^{3+} were studied over both batch and continuous cultures using the STR. The batch cultivation was run for 96 h to allow the bacteria to grow and produce the maximum amount of Fe^{3+} (9-10 g/l) as shown in Fig. 2. The stirring conditions of the STR at various phases were dictated by preliminary tests (not shown) and corresponded to maximum production of Fe^{3+} at negligible mass transfer and bacteria damage limitations. Batch cultivation provided a stabilised environment for acclimatisation in a high level of activity before transitioning to the continuous phase. When continuous cultivation was started, the hydraulic residence time was decreased from 96 h to 24 h driven by the high oxidation rate of Fe^{2+} and the fast growth of bacteria supported by the consistent addition of fresh nutrients at a flow rate of 10.41 ml/h (250 ml/day). In the beginning, a sufficiently long HRT was required to achieve high Fe^{3+} concentrations and a high iron oxidation efficiency for high efficiency of the leaching process specially at high pulp densities as the regeneration of Fe^{3+} in the solution was avoided. The continuous rate for iron oxidation was 2.81 g/l d with HRT of 96 h which was increased to 11.25 g/l d with HRT of 24 h with a maximum concentration of 11.5 g/l. Different iron oxidation rates have been reported in iron-oxidizing bioreactors operated at continuous flow. For instance, Kaksonen et al., (2014a) achieved an iron oxidation rate of 16.3 g/l d at an HRT of 8 h with a maximum Fe^{3+} concentration of 14.1 g/l and Hubau et al., (2018) reported an iron oxidation rate of 7.82 g/l d at an HRT of 48 h and a maximum Fe^{3+} concentration of 8 g/l. Table 2 provides an overview of the continuous iron oxidation experiments performed in STR using acidophilic bacteria, emphasising the relationship between the HRT, Fe^{3+} concentration and oxidation rate.

Fig. 2. shows the profiles of the continuous bio-oxidation of Fe^{2+} to Fe^{3+} in STR over 220 h by the bacterium *A. ferrooxidans*. In the first 48 h, the bacteria were in a lag phase, as evidenced by the low Fe^{3+} concentration (below 2 g/l) and the high Fe^{2+} concentration (above 10 g/l), reflecting the time that would be required for the bacteria to acclimate to the reactor environment and initiate metabolic activity. Following the lag phase, Fe^{3+} production entered the logarithmic phase, with concentrations exceeding 7 g/l and demonstrating the rapid consumption of Fe^{2+} Eq. (1). As the continuous culture process started, Fe^{3+} production increased further from 7.5 g/l to over 10 g/l, while the Fe^{2+} concentration dropped significantly below 2 g/l. The pH also increased from 1.7 to 2 owing to the biooxidation associated with the consumption of H^+ and Eh reached 510 mV. Between 120 and 220 h, the steady-state phase was achieved, where Fe^{3+} production remained stable within the range of 10.5–11.5 g/l. In this phase, the rates of substrate consumption and product formation were balanced, resulting in a stable operational environment. Maintaining a convenient environment by setting parameters for the bacteria such as pH, temperature, aeration, and nutrient supply, is essential for sustaining the steady-state phase.

3.2. Batch leaching of Cu

The batch indirect leaching using biogenic Fe^{3+} (without bacteria) was conducted in a flask scale to figure out the pulp density without compromising the Cu leaching efficiency. The pulp density is one of the important parameters that affect the reactor design, the culture media consumption and overall operating cost (Zhang et al., 2020). As shown in Fig. 3(a), the leaching efficiency of Cu after 96 hours decreased remarkably with increasing pulp density owing to the limited availability of Fe^{3+} in the solution to dissolve higher concentrations of Cu. Moreover, the hydrolysis of Fe^{3+} and the formation of jarosite precipitate Eq. (3) were competing with of the reduction of Fe^{3+} to Fe^{+2} Eq. (2). Jarosite deposited on the surface of PCB powder as a passivation layer and prevented the direct contact of Fe^{3+} with the PCB powder as confirmed by XRD analysis in section 3.5 (Chen et al., 2015; Maluleke et al., 2024). Although increasing the Fe^{3+} concentration would have improved the leaching efficiency, as demonstrated in other studies (Tapia et al., 2022), this approach was not pursued for economic considerations due to the consumption of ferrous sulphate. As a result, the experiment focused on examining other important parameters for efficient leaching.

$$3Fe^{3+} + 2HSO_4^- + 6H_2O + M^+ \rightarrow MFe_3(SO_4)_2(OH)_6 + 8H^+ \quad [M: K^+, NH_4^+] \tag{3}$$

There was a sharp decrease in the leaching rate from 97.94% at a pulp density of 1% to 35.5% at a pulp density of 8%. At high pulp densities, the concentration of Cu increased which means more agents were required to leach Cu and highlights the critical role of Fe^{3+} in the leaching of Cu. When Fe^{3+} became insufficient, the leaching efficiency dropped significantly. Approximately half of Cu was leached at a pulp density of 6%, leading to a potential to enhance the leaching efficiency by a parametric study of the operation of the continuous leaching reactor. The pulp density of 6% was chosen for the continuous leaching study. The pH variation at various pulp densities is shown in Fig. 3(b). The biogenic Fe^{3+} solution had an initial pH of ~1.9. During the leaching however, the pH increased due to the alkalinity of the waste powder, the reduction of Fe^{3+} to Fe^{2+} Eq. (2) and the precipitation Eq. (3) (Işıldar et al., 2016). Higher pulp density resulted in more consumption of H^+ ions which raised the pH of the solution. At a pulp density of 1%, the pH had a slight increase to around 2.2 but reached 2.5 and 3.2 at pulp density values of 2% and 4%, respectively. At a pulp density of 6%, the pH level was approximately 3.5 while at the maximum pulp density (8%), the pH exceeded 4. These findings demonstrate the importance of controlling the pH level and the pulp density for efficient Cu leaching.

Table 3 lists some representative examples of the use of pulp densities, ranging from 3.5% to 10%, in the bioleaching processes of wastes under different conditions by a single microorganism or consortium of microorganisms. In some cases, high pulp densities required more days to leach the metals.

3.3. Copper leaching in a continuous mode

3.3.1. pH adjustment

The continuous bioleaching experiments were carried out using an initial concentration of 10-11.5 g/l of the obtained biogenic Fe^{3+} derived from the continuous bioreactor after the removal of the bacteria. The impact of the key operating parameters, including pH, temperature and residence time on the leaching rate of Cu was investigated. Fig. 4(a) illustrates effect of the pH adjustment, by adding sulphuric acid 98% to maintain a pH below 2 (~ 1.7), on the leaching rate of Cu at a pulp density of 6%, HRT of 96 h and 40 °C. The pH played a non-negligible role in the leaching rate owing to impact of excess in H^+ on the re-oxidation of Fe^{2+} to Fe^{3+} (Boxall et al., 2018; Hubau et al., 2018). For example, Iglesias-González et al., (2024) achieved a 99% Cu leaching rate by adjusting the pH to below 1.5 at a pulp density ranging from 0.25% to 1.75% and HRT of 6 h. Approximately 43% of Cu was leached after just 24 h in the pH-adjusted samples, compared to only 22% in samples without pH adjustment. Over the 96 h, complete leaching (100%) was achieved with pH adjustment whilst 80% of Cu was leached in the absence of pH control, highlighting the importance of maintaining a controlled acidic environment suitable for the solubility of metal ions (Boxall et al., 2018; Maluleke et al., 2024). Fig. 4(b) shows the profiles of pH and Eh in the samples with and without pH adjustment. In the sample with pH adjustment (pH 1), pH level was increased after 24 h and maintained to around 1.9 by sulphuric acid addition, while in sample without pH adjustment (pH 2), pH level increased gradually and reached 3 after 96 h of leaching. These profiles were fundamentally influenced by the alkalinity of waste PCBs (Brandl et al., 2001). The Eh also showed the same trend as the trend of pH. In the pH-adjusted samples (Eh 1), Eh decreased from 350 to 300 mV after 24 h of leaching due to Fe^{3+} consumption Eq. (2) and increased after sulphuric acid addition Eq. (1). In contrast, in samples without pH adjustment (Eh 2), the Eh gradually decreased throughout the experiment, reaching near 200 mV after 96 h. The opposite trend of the relationship between pH and Eh validates the fact that there were insufficient H^+ ions and Fe^{3+} as oxidising agents. When Eh went down, the ability of a solution to oxidize decreased, which demonstrates the importance of keeping pH levels controlled for effective bioleaching (Willner, 2013). The dissolution rate during the leaching is displayed in Table 4. In samples with pH adjustment, the dissolution rate increased significantly up to the second day. The increasing trend is clearly illustrated in Fig. 4(a), where the leaching rate reached approximately 80% after 48 h. On the 72 and 96 h however, the dissolution rate dropped sharply, and the leaching rate increased gradually to above 85% and ultimately reached 100% in 96 h. The dissolution rate in 96 h was minimal compared to the initial hours, demonstrating the dissolution of most of the metallic Cu in first days. The dissolution rate in samples without pH control was lower than that of pH adjusted samples. In 24 and 48 h of the leaching, the dissolution rate was about half of the pH-adjusted samples, which is seen in Fig. 4(a) where the leaching rate after 48 h was around 45%, compared to around 80% in sample with pH adjustment. As opposed to the conventional chemical acid leaching or direct bioleaching processes, which require significantly low pH levels for the benefit of bacterial survival, the results herein prevented the formation of jarosite by the addition of small amounts of acid for pH adjustment, which validated the requirement of embedding a fast response pH sensor for the continuous control of acidity while the HRT of the leaching was extended to several days.

3.3.2. Effect of temperature

The leaching rate of Cu by Fe^{3+} ions as a function of the reaction temperature is presented in Fig. 5(a). The higher temperature favoured the process compared to the room temperature which did not exceed 50% at room temperature and after 96 h of operation, validating the shift of the chemical equilibrium towards high conversion favoured by the endothermic nature of the leaching process. Temperature affected the kinetic of the leaching, as observed in the intermediate time value in Fig. 5(a), by accelerating predominantly the reaction rates of Eq. (2), through exponential trends following classical Arrhenius plot, than associated mass transports by diffusion in the pores of the PCB particles and convective mixing in the leaching medium through linear trend, thereby affecting the transient solubility of metals (Bahaloo-Horeh and Mousavi, 2022; Faraji et al., 2022). As shown in table 5, Cu concentration after leaching was 5,850 mg/l, while at 40 °C it increased to 12,550 mg/l. The effect of temperature on bioleaching has been investigated in several studies. For example, Wang et al., (2015) reported that bioleaching of Cu at room temperature was 84%, compared to 91% at 35 ℃ for 90 days. Tanda., (2017) showed 32 % Au was leached at 60 °C while only 0.5 % was leached at 25 °C from low grade copper-gold ore. In another study, You et al., (2020) carried out the bioleaching in a series of three CSTRs and indicated that after 7 days the bioleaching rate of Cu increased from 34.8% to 49.3% in the first CSTR, 40.3% to 71.2% in the second CSTR, and 44.3% to 73.8% in the third CSTR, with increasing temperature from 30 to 37. Employing indirect leaching allowed flexibility to adapt temperature to the desired rate with reduced concern about the bacterial survival and energy costs observed in the direct leaching, as temperature above the optimal microbial growth condition could have lysed the microbial cell and adversely affected the metal dissolution (Parsa et al., 2024). The apparent activation energy (E_a) of 59.87 kJ/mol, estimated at similar leaching rates based on Eq. (4) (Levenspiel, 1999) and temperatures T_1 (293 K) and T_2 (313 K) corresponding to times t_1 (96 h) and t_2 (24 h), respectively, was close to the one cited by You et al., (2020), validating the relevance of chemical mechanism in controlling the overall kinetics of the bioleaching process at the surface and inside the pores of particles of PCBs.

$$ln t_1/t_2 = E_a/R(1/T_1 - 1/T_2) \tag{4}$$

3.3.3. Effect of the hydraulic residence time (HRT)

The results of leaching experiments conducted at various HRT under two conditions, with and without pH adjustment, are presented in Fig. 5(b). The HRT was set at 48 and 96 h to allow sufficient time for Fe^{3+} to be consumed in the solution and facilitate the dissolution of Cu. The findings reveal a significant influence of HRT on the rate since in the samples with longer HRT a higher dissolution of Cu was observed, regardless of whether the adjustment of pH was applied, facilitated by a longer contact of the leaching agent with the waste. This is also evident in Table 5, where a longer HRT resulted in higher Cu concentrations after leaching (11,000 mg/l), even without pH control. The highest dissolution rate in HRT of 48 h was 76.68% when pH adjusted below 2. In contrast, the same HRT without pH control resulted in the lowest dissolution rate (62.17%). At an HRT of 96 h, approximately 84% of Cu was leached, demonstrating the effect of HRT, and by inference the kinetically controlled regime, in extending interaction between the leaching agent (Fe^{3+}) and Cu in the solution. The ICP analysis of the leaching solution revealed the presence of other metals such as Ni, Mg and Al with less proportions (Table 6). Cu was found however to be the most abundant, with a concentration of 193.06 mg per gram of PCB powder, offering a promising leaching yield even at high pulp density, and thus an economic viability for the recovery. Expansion to the recovery of other metals is being considered by the ongoing works by the authors.

3.3.4. Species thermodynamic stability

The Eh-pH plot by the Pourbaix diagram was used to validate the thermodynamic stability of solubility of the species in the solution under a range of pH and Eh values. Fig. 6 depicts the Pourbaix diagram of the Fe-SO_4 and Fe-Cu system at 25°C estimated by Hydra-Medusa software (Version 3, developed by the Royal Institute of Technology (KTH) and the concentration of sulphate in the leaching solution was determined using the turbidimetric method (Rossum and Villarruz, 1961). Fig. 6a reveals a wide range for the precipitation of Fe^{3+} ions as a jarosite, particularly for pH value above 2 and Eh value up to 0.25 V. Under the acidic and reducing conditions, solid complexes such as Fe_3S_4 dominates, which interferes with the copper leaching by removal of the Fe^{3+} ions from the solution, highlighting a careful control of the Eh-pH that minimises the deposition of jarosite and associated insoluble species. Fig. 6b shows Pourbaix diagram of Cu in aqueous solution where different Cu and its derivative oxide species exist depending on the Eh and pH values of the solution. Generally, it is observed that an operation at low pH and high Eh facilitates soluble Cu in the solution. At thermodynamic equilibrium, most of the leached Cu exists as soluble Cu^{2+} compound for pH values below 3.2 and Eh values above 0.75 V. The diagram also shows that exposition to an atmosphere of air undergoes reaction with O_2 to form oxides of various oxidation states, depending on the operating conditions (i.e. concentration of oxides and partial pressure of oxygen gas and pH of the solution), which has also been reported by (Puigdomenech and Taxén, 2000). Under reducing conditions, Cu may remain in its metallic state. Since Cu concentration is a critical variable, an average concentration of 132 mM from the leaching solution was used. Based on Fig. 6c, Fe can be present as Fe^{2+} in the solution even at neutral pH and Eh value ranging from -0.5 to 0.25 V. It should be noted that in the leaching solution, the concentration of Fe^{2+} is a critical objective to reduce the cost of the process as it can be recycled back to the bioreactor and used as a nutrient to feed the bacteria (Maluleke et al., 2024).

3.4. Characterisation of solid samples

3.4.1. XRD analysis

XRD patterns of PCB powder were analysed at three stages: initial powder before bioleaching Fig. 7(a), after batch leaching for 96 h Fig. 7(b), and after continuous leaching without pH control for 96 h Fig. 7(c). In the pre-leached powder Fig. (7a), the high peaks between 27.23° and 32.62° with intensity values of 13,527, 12,963, and 12,836 reveal the presence of metals such as Cd, Pb, Sn, Cu and Se. The peaks between 40 to 50° with the highest peak at 43.94° attributed to the presence of Al and Fe. The peak at 51.01° with an intensity of 11517 shows the existence of metals like Cu, and Pb (Panda et al., 2020). After the batch leaching, the peaks between 10° and 20° and 40° to 50° identified the formation of jarosite owing to the increase in the pH above 3.3, and such trap of Cu in the jarosite resulted in a lower leaching rate in alignment the result reported in the literature (Tapia et al., 2022). The high peak at 27° indicates the presence of metals such as the anticipated Fe and Ni deposits, followed by the peaks within the 30° to 40° range which indicate the presence of Co and Mg. After the continuous leaching, the presence of Ag, Mg and Ni is observed at the peaks from 20° to 30°. The large peaks at 30° to 50° show some un-leached metals such as Al, Pb, Sn and Mg.

3.4.2. FE-SEM analysis

FE-SEM and EDX- mapping by microscopic imaging are shown in Fig. 8(a)-(c) for the pre-leached waste PCB Fig. 8(a), residue powder after the batch leaching in a flask Fig. 8(b) and the residue powder after the continuous leaching in STR without pH control Fig. 8(c), respectively. The images were captured at two magnifications to access to further details in the morphological changes of the surface during the leaching process. As seen in Fig. 8(a), the initial powder was not flat, had a rod and spherical structures with rough surface and exhibited a relatively large particle size. After the leaching, there were changes in size, shape and structure of the powder that turned into a granular shape with a smooth surface, confirming the leaching of Cu from both the surface area and the pores of the PCBs over the redox reaction with the leaching agent (Fe^{3+}). EDX-mapping of residue powder confirms the removal of Cu from the powder during both batch and continuous leaching associated with an increased concentration of precipitated Fe^{3+} as jarosite.

3.5. Cu recovery via Electrowinning

The Cu rich solution obtained from the indirect continuous leaching with a pulp density of 6% without pH adjustment at 40 °C after 96 h was subjected to electrowinning for metal Cu purification. As illustrated in Fig. 9(a), the mass of deposited Cu on the cathode increased with the electrowinning time and approximately 70.85% of the leached Cu was recovered. The experimental results were compared with the theoretical values estimated according to the Faraday law Eq. (5):

$$w = {}^{itM}\!/_{zF} \tag{5}$$

Where w represents the mass of deposited Cu (g), i is the current (A), t is the electrowinning time (s), M is the molecular weight of Cu, z is the electron number (2 for Cu) and F is Faraday constant (96,485 C/mol)). As seen, during the initial 2 h, the practical mass of deposited Cu was quite close to the theoretical value but from the 3 h onward, the mass of Cu in the experiment fell below the theoretical value and the efficiency dropped to 69% after 4 h and reached 52% after 8 h, indicating the decrease in the available Cu in the solution. The dissolved Cu^{2+} in the leachate was reduced to metallic Cu or copper oxide on the cathode surface, according to Eqs. (6)-(8), where E^{o} is the standard reduction potential. At the same time, water oxidation occurs at the anode according to the reaction by equation Eq. (9) (Fathima et al., 2022).

$$Cu^{2+} + 2e^{-} \rightarrow Cu_{(s)} \qquad E^0 = 0.337\,V \tag{6}$$

$$Cu^{+} + e^{-} \rightarrow Cu_{(s)} \qquad E^0 = 0.506\,V \tag{7}$$

$$2Cu^{2+} + H_2O + 2e^{-} \rightarrow Cu_2O_{(s)} + 2H^{+} \qquad E^0 = 0.207\,V \tag{8}$$

$$H_2O \rightarrow \frac{1}{2}O_2 + 2H^{+} + 2e^{-} \tag{9}$$

Fig. 9(b)-(d). shows the gradual accumulation of Cu on the cathode surface over time. As the electrowinning process proceeded, Cu deposit changed and became darker and rougher. Some studies have cited the recovery of Cu after the bioleaching process. For instance, Fathima et al., (2022) demonstrated the maximum metal deposition values for Au (97.33%), Ag (81.57%) and Cu (90.35%) after 12 h of electrowinning time. The presence of other metals in the leachate with reduction potentials more positive than Cu (i.e. reduction potential: 0.34 V) was not observed to contribute to the deposition at the cathode. Meanwhile, metals with negative reduction potentials such as Al (-1.6 V), Ni (-0.26 V), Fe (-0.45 V), and Mg (-2.37 V) and less concentration compared to Cu (Table 6) remained in solution, which made the deposition of metals other than Cu unlikely (Baniasadi et al., 2021).

After completing the electrowinning, the Cu foil was manually removed from the cathode surface (as shown in Fig. 9(e)) and the purity of the deposited Cu was observed using the EDX analysis (Fig. 9(f)). The results revealed a high purity of Cu (86.76%), with a small portion of Al (1.08%), Si (1.69%) and Ca (0.92%). A small amount of oxygen (2.86%) was identified, which can be attributed to the copper oxide composition. Out of the total 2.48 g of solid metal deposited on the cathode surface, 2.15 g was Cu, 0.0228 g was Ca, 0.0419 g was Si and 0.0267 was Al, showing the efficiency of the electrowinning process to recover a highly pure Cu.

4. Conclusion

In the present work, the two-step indirect bioleaching coupled with the recovery of pure Cu from waste PCBs was demonstrated as a green and environmentally friendly route for efficient processing at flexible operating conditions. The continuous cultivation of the bacterium *Acidithiobacillus ferrooxidans* in the 1.5 L stirred tank reactor produced ferric iron (Fe^{3+}) at high concentration (10.5–11.5 g/l), which ensured a consistent supply of Fe^{3+} for the following leaching step. The pulp density of 6% w/v of PCB load resulted in 50.7% Cu at 40 °C for 96 h of batch operation and was used then as reference for the leaching in a continuous stirred tank reactor. The parametric study highlighted the role of controlled pH, temperature and hydraulic residence time for a complete leaching rate of Cu at reduced feed and energy costs. The results showed that maintaining an acidic environment (pH ~1.7) significantly enhanced the leaching efficiency, with a complete leaching rate within 96 h at 40 °C. A longer hydraulic residence time (HRT) was shown to have a positive effect on Cu leaching even without pH adjustment by allowing sufficient contact between the leaching agent and PCB particles, leading to higher dissolution rates. High Temperature also increased the leaching rate by enhancing reaction kinetics and doubling the Cu concentration in the leachate at 40 °C compared to that at room temperature. The Pourbaix diagrams confirmed the thermodynamic equilibria between various species of Cu and iron oxides by maintaining low pH and high Eh to stabilise soluble Cu^{2+} species and minimise the precipitation of Fe^{3+} as jarosite. The analysis of the residual powder by XRD, FE-SEM and EDX helped understand the morphological changes on surfaces of PCBs, aligning with the results by ICP-OES. Further purification by the electrowinning process enabled a recovery of 70.85% of pure Cu from metal rich solution. This two-step indirect approach enabled the processing of high PCB loads (6 % w/v) under continuous operations, offering a route of intensifying the process operations at reduced energy consumption and thus opening new perspectives towards the large-scale e-waste recycling.

Acknowledgement

Authors acknowledge the support of Innovate UK, KTP012187, and ICT Reverse Asset Management Ltd for the financial supports of this work.

Reference:

Adam, F., Piret, A., Canonne, M., Decock, R., Nicolay, X., 2024. Complete recycling of Printed Circuit Boards: From base metal bioleaching in a semi-continuous reactor with dual regulation to gold biosorption with brewer's yeast. Hydrometallurgy. 223, 106190. https://doi.org/10.1016/j.hydromet.2023.106190.

Arshadi, M., Pourhossein, F., Mousavi, S. M., Yaghmaei, S., 2021. Green recovery of Cu-Ni-Fe from a mixture of spent PCBs using adapted *A. ferrooxidans* in a bubble column bioreactor. Sep. Purif. Technol. 272, 118701. https://doi.org/10.1016/j.seppur.2021.118701. Arshadi, M and Yaghmaei, S., 2020. Advances in bioleaching of copper and nickel from electronic waste using *Acidithiobacillus ferrooxidans*: evaluating daily pH adjustment. Chemical Papers. 74, 2211-2227. https://doi.org/10.1007/s11696-020-01055-y.

Arslan, V., 2021. Bacterial leaching of copper, zinc, nickel and aluminum from discarded printed circuit boards using acidophilic bacteria. J. Mater. Cycles. Waste. Manag. 23, 2005-2015. https://doi.org/10.1007/s10163-021-01274-9.

Arya, S., Kumar, S., 2020. Bioleaching: urban mining option to curb the menace of Ewaste challenge. Bioengineered. 11, 640–660. https://doi.org/10.1080/21655979.2020.1775988.

Bahaloo-Horeh, N., Mousavi, S. M., 2022. A novel green strategy for biorecovery of valuable elements along with enrichment of rare earth elements from activated spent automotive catalysts using fungal metabolites. J. Hazard. Mater. 430, 128509. https://doi.org/10.1016/j.jhazmat.2022.128509.

Baniasadi, M., Graves, J. E., Ray, D. A., De Silva, A. L., Renshaw, D., Farnaud, S., 2021. Closed-loop recycling of copper from waste printed circuit boards using bioleaching and electrowinning processes. Waste. Biomass. Valori. 12, 3125-3136. https://doi.org/10.1007/s12649-020-01128-9.

Becci, A., Amato, A., Rodriguez-Maroto, J. M., Beolchini, F., 2021. Bioleaching of end-of-life printed circuit boards: Mathematical modeling and kinetic analysis. Ind. Eng. Chem. Res. 60, 4261-4268. https://doi.org/10.1021/acs.iecr.0c05566.

Boxall, N.J., Cheng, K.Y., Bruckard, W., Kaksonen, A.H., 2018. Application of indirect non-contact bioleaching for extracting metals from waste lithium-ion batteries. J. Hazard. Mater. 360, 504–511. https://doi.org/10.1016/j.jhazmat.2018.08.024.

Brandl, H., Bosshard, R., Wegmann, M., 2001. Computer-munching microbes: metal leaching from electronic scrap by bacteria and fungi. Hydrometallurgy. 59, 319-326. https://doi.org/10.1016/S0304-386X(00)00188-2.

Bryan, C. G., Watkin, E. L., McCredden, T. J., Wong, Z. R., Harrison, S. T. L., Kaksonen, A. H., 2015. The use of pyrite as a source of lixiviant in the bioleaching of electronic waste. Hydrometallurgy. 152, 33-43. https://doi.org/10.1016/j.hydromet.2014.12.004 .

Cancho, L., Blázquez, M. L., Ballester, A., González, F., Muñoz, J. A., 2007. Bioleaching of a chalcopyrite concentrate with moderate thermophilic microorganisms in a continuous reactor system. Hydrometallurgy. 87, 100-111. https://doi.org/10.1016/j.hydromet.2007.02.007.

Chen, S. Y., Wu, J. Q., Sung, S., 2022. Effects of sulfur dosage on continuous bioleaching of heavy metals from contaminated sediment. J. Hazard. Mater. 424, 127257. https://doi.org/10.1016/j.jhazmat.2021.127257.

Chen, S., Yang, Y., Liu, C., Dong, F., Liu, B., 2015. Column bioleaching copper and its kinetics of waste printed circuit boards (WPCBs) by *Acidithiobacillus ferrooxidans*. Chemosphere. 141, 162-168. https://doi.org/10.1016/j.chemosphere.2015.06.082.

Dong, Y., Zan, J., Lin, H., 2023. Recovery of precious metals from waste printed circuit boards though bioleaching route: A review of the recent progress and perspective. J. Environ. Manage. 348, 119354. https://doi.org/10.1016/j.jenvman.2023.119354.

Erust, C., Akcil, A., Tuncuk, A., Panda, S., 2020. Intensified acidophilic bioleaching of multi-metals from waste printed circuit boards (WPCBs) of spent mobile phones. J. Chem. Technol. Biotechnol. 95, 2272-2285. https://doi.org/10.1002/jctb.6417.

Faraji, F., Alizadeh, A., Rashchi, F., Mostoufi, N., 2022. Kinetics of leaching: A review. Rev. Chem. Eng. 38, 113-148. https://doi.org/10.1515/revce-2019-0073.

Fathima, A., Tang, J. Y. B., Giannis, A., Ilankoon, I. M. S. K., Chong, M. N., 2022. Catalysing electrowinning of copper from E-waste: A critical review. Chemosphere. 298, 134340. https://doi.org/10.1016/j.chemosphere.2022.134340.

Gericke, M., Govender, Y., Pinches, A., 2010. Tank bioleaching of low-grade chalcopyrite concentrates using redox control. Hydrometallurgy, 104, 414-419. https://doi.org/10.1016/j.hydromet.2010.02.024.

Gómez, J., Cantero, D., 2003. Kinetic study of biological ferrous sulphate oxidation by iron-oxidising bacteria in continuous stirred tank and packed bed bioreactors. Process. Biochem. 38, 867-875. https://doi.org/10.1016/S0032-9592(02)00048-1.

Guo, X., Chen, S., Han, Y., Hao, C., Feng, X., Zhang, B., 2023. Bioleaching performance of vanadium-bearing smelting ash by *Acidithiobacillus ferrooxidans* for vanadium recovery. J. Environ. Manage. 336, 117615. https://doi.org/10.1016/j.jenvman.2023.117615.

Hosseini Nasab, M., Noaparast, M., & Abdollahi, H. (2021). Direct and indirect bio-leaching of Co and Ni from an iron-rich laterite ore using *Delftia acidovorans* and *Acidithiobacillus ferrooxidans*. J. Min. Environ. 12, 471-489. https://doi.org/10.22044/jme.2021.10528.2002.

Hubau, A., Minier, M., Chagnes, A., Joulian, C., Perez, C., Guezennec, A. G., 2018. Continuous production of a biogenic ferric iron lixiviant for the bioleaching of printed circuit boards (PCBs). Hydrometallurgy. 180, 180-191. https://doi.org/10.1016/j.hydromet.2018.07.001.

Hubau, A., Minier, M., Chagnes, A., Joulian, C., Silvente, C., Guezennec, A. G., 2020. Recovery of metals in a double-stage continuous bioreactor for acidic bioleaching of printed circuit boards (PCBs). Sep. Purif. Technol. 238, 116481. https://doi.org/10.1016/j.seppur.2019.116481.

Iglesias-González, N., Dorado, A. D., Ramírez, P., Mazuelos, A., 2024. A high productivity bioprocess for obtaining metallic copper from printed circuit boards (PCBs). Miner. Eng 205, 108459. https://doi.org/10.1016/j.mineng.2023.108459.

Ilkhani, Z., Vakilchap, F., Sadeghi, N., Mousavi, S. M., 2024. Base metals (Fe, Al, Ti) and rare earth elements (Ce, La, Pr) leaching from red mud through an efficient chemical-biological hybrid approach. Miner. Eng. 208, 108603. https://doi.org/10.1016/j.mineng.2024.108603.

Ilyas, S., Lee, J. C., Chi, R. A., 2013., Bioleaching of metals from electronic scrap and its potential for commercial exploitation. Hydrometallurgy. 131, 138-143. https://doi.org/10.1016/j.hydromet.2012.11.010.

Işıldar, A., van de Vossenberg, J., Rene, E. R., van Hullebusch, E. D., Lens, P. N., 2016. Two-step bioleaching of copper and gold from discarded printed circuit boards (PCB). J. Waste. Manag. 57, 149-157. https://doi.org/10.1016/j.wasman.2015.11.033.

Kaksonen, A. H., Morris, C., Hilario, F., Rea, S. M., Li, J., Usher, K. M., du Plessis, C., 2014a. Iron oxidation and jarosite precipitation in a two-stage airlift bioreactor. Hydrometallurgy. 150, 227-235. https://doi.org/10.1016/j.hydromet.2014.05.020.

Kaksonen, A. H., Morris, C., Rea, S., Li, J., Wylie, J., Usher, K. M., du Plessis, C. A., 2014b. Biohydrometallurgical iron oxidation and precipitation: part I—effect of pH on process performance. Hydrometallurgy. 147, 255-263. https://doi.org/10.1016/j.hydromet.2014.04.016.

Karamanev, D. G., Nikolov, L. N., Mamatarkova, V., 2002. Rapid simultaneous quantitative determination of ferric and ferrous ions in drainage waters and similar solutions. Miner. Eng. 15, 341-346. https://doi.org/10.1016/S0892-6875(02)00026-2.

Levenspiel, O., 1998. Chemical reaction engineering, third ed. John wiley and sons Inc, New York.

Mäkinen, J., Bachér, J., Kaartinen, T., Wahlström, M., Salminen, J., 2015. The effect of flotation and parameters for bioleaching of printed circuit boards. Miner. Eng. 75, 26-31. https://doi.org/10.1016/j.mineng.2015.01.009.

Mahmoud, A., Cézac, P., Hoadley, A. F., Contamine, F., d'Hugues, P., 2017. A review of sulphide minerals microbially assisted leaching in stirred tank reactors. Int. Biodeter. Biodegr. 119, 118-146. https://doi.org/10.1016/j.ibiod.2016.09.015.

Maluleke, M. D., Kotsiopoulos, A., Govender-Opitz, E., Harrison, S. T., 2024. Bioleaching of printed circuit boards in a two-stage reactor system with enhanced ferric iron regeneration in a re-circulating packed-bed reactor from PCB leaching. Miner. Eng. 218, 109000. https://doi.org/10.1016/j.mineng.2024.109000.

Ojumu, T. V., Petersen, J., 2011. The kinetics of ferrous ion oxidation *by Leptospirillum ferriphilum* in continuous culture: The effect of pH. Hydrometallurgy. 106, 5-11. https://doi.org/10.1016/j.hydromet.2010.11.007.

Pakostova, E., Herath, A., 2023. A bioleaching process for sustainable recycling of complex structures with multi-metal layers. Sustainability. 15, 14068. https://doi.org/10.3390/su151914068.

Panda, R., Jadhao, P. R., Pant, K. K., Naik, S. N., Bhaskar, T., 2020. Eco-friendly recovery of metals from waste mobile printed circuit boards using low temperature roasting. J. Hazard. Mater. 395, 122642. https://doi.org/10.1016/j.jhazmat.2020.122642.

Parsa, A., Bahaloo-Horeh, N., Mousavi, S. M., 2024. A kinetic study of indium, aluminum, arsenic, and strontium extraction from LCDs using biometabolites produced by *Aspergillus* niger. Miner. Eng. 205, 108441. https://doi.org/10.1016/j.mineng.2023.108441.

Pathak, A., Kothari, R., Dastidar, M. G., Sreekrishnan, T. R., Kim, D. J., 2014. Comparison of bioleaching of heavy metals from municipal sludge using indigenous sulphur and iron-oxidizing microorganisms: Continuous stirred tank reactor studies. J. Environ. Sci. Heal. A. 49, 93-100. https://doi.org/10.1080/10934529.2013.824737.

Pradhan, J.K., Kumar, S., 2012. Metals bioleaching from electronic waste by *Chromobacterium violaceum* and *Pseudomonads* sp. Waste. Manag. Res. 30, 1151–1159. https://doi.org/10.1177/0734242X12437565.

Priya, A., Hait, S., 2017. Comparative assessment of metallurgical recovery of metals from electronic waste with special emphasis on bioleaching. Environ. Sci. Pollut. Res. 24, 6989-7008. https://doi.org/10.1007/s11356-016-8313-6.

Puigdomenech, I., Taxén, C., 2000. Thermodynamic data for copper. Implications for the corrosion of copper under repository conditions (No. SKB-TR--00-13). Swedish Nuclear Fuel and Waste Management Co.

Reynier, N., Gagné-Turcotte, R., Coudert, L., Costis, S., Cameron, R., Blais, J. F., 2021. Bioleaching of uranium tailings as secondary sources for rare earth elements production. Minerals. 11, 302. https://doi.org/10.3390/min11030302.

Rodrigues, M. L., Leão, V. A., Gomes, O., Lambert, F., Bastin, D., Gaydardzhiev, S., 2015. Copper extraction from coarsely ground printed circuit boards using moderate thermophilic bacteria in a rotating-drum reactor. J. Waste. Manag. 41, 148-158. https://doi.org/10.1016/j.wasman.2015.04.001.

Rossum, J. R., Villarruz, P. A., 1961. Suggested method for turbidimetric determination of sulfate in water. J. Am. Water. Works. Ass. 53, 873-876. https://doi.org/10.1002/j.1551-8833.1961.tb00723.x.

Sadeghi, N., Vakilchap, F., Ilkhani, Z., Mousavi, S. M., 2024. Assessment of the visible light effect on one-step bacterial leaching of metals from spent lithium-ion batteries cathode pretreated by a bio-chemical lixiviant. J. Clean. Prod. 436, 140432. https://doi.org/10.1016/j.jclepro.2023.140432.

Shin, D., Jeong, J., Lee, S., Pandey, B. D., Lee, J. C., 2013. Evaluation of bioleaching factors on gold recovery from ore by cyanide-producing bacteria. Miner. Eng. 48, 20-24. https://doi.org/10.1016/j.mineng.2013.03.019.

Tanda, B. C. 2017. Glycine as a lixiviant for the leaching of low grade copper-gold ores (Doctoral dissertation, Curtin University). http://hdl.handle.net/20.500.11937/56525.

Tapia, J., Dueñas, A., Cheje, N., Soclle, G., Patiño, N., Ancalla, W., Lazarte, A., 2022. Bioleaching of heavy metals from printed circuit boards with an acidophilic iron-oxidizing microbial consortium in stirred tank reactors. Bioengineering. 9, 79. https://doi.org/10.3390/bioengineering9020079.

Trivedi, A., Hait, S., 2023. Metal bioleaching from printed circuit boards by bio-Fenton process: Optimization and prediction by response surface methodology and artificial intelligence models. J. Environ. Manage. 326, 116797. https://doi.org/10.1016/j.jenvman.2022.116797.

Van Yken, J., Cheng, K. Y., Boxall, N. J., Nikoloski, A. N., Moheimani, N., Valix, M., Kaksonen, A. H., 2023. An integrated biohydrometallurgical approach for the extraction of base metals from printed circuit boards. Hydrometallurgy. 216, 105998. https://doi.org/10.1016/j.hydromet.2022.105998.

Vardanyan, A., Vardanyan, N., Aâtach, M., Malavasi, P., Gaydardzhiev, S., 2022a. Bio-Assisted Leaching of Non-Ferrous Metals from Waste Printed Circuit Boards—Importance of Process Parameters. Metals. 12, 2092. https://doi.org/10.3390/met12122092.

Vardanyan, A., Vardanyan, N., Abrahamyan, N., Aatach, M., Gaydardzhiev, S., 2022b. Sequential biologically assisted extraction of Cu and Zn from printed circuit boards (PCB). Int. J. Environ. 1-16. https://doi.org/10.1080/00207233.2022.2126122.

Wang, J., Hu, M. H., Zhao, H. B., Tao, L., Gan, X. W., Qin, W. Q., Qiu, G. Z., 2015. Well-controlled column bioleaching of a low-grade copper ore by a novel equipment. J. Cent. South. Uni. 22, 3318-3325. https://doi.org/10.1007/s11771-015-2872-4.

Willner, J., 2013. Influence of physical and chemical factors on biological leaching process of copper from printed circuit boards. Metalurgija. 52, 189-192. https://hrcak.srce.hr/92534.

Xia, M. C., Wang, Y. P., Peng, T. J., Shen, L., Yu, R. L., Liu, Y. D., Zeng, W. M., 2017. Recycling of metals from pretreated waste printed circuit boards effectively in stirred tank reactor by a moderately thermophilic culture. J. Biosci. Bioeng. 123, 714-721. https://doi.org/10.1016/j.jbiosc.2016.12.017.

Xin, B., Jiang, W., Li, X., Zhang, K., Liu, C., Wang, R., Wang, Y., 2012. Analysis of reasons for decline of bioleaching efficiency of spent Zn–Mn batteries at high pulp densities and exploration measure for improving performance. Bioresour. Technol. 112, 186-192. https://doi.org/10.1016/j.biortech.2012.02.133.

Xu, P., Yang, Z., Yu, X., Holoubek, J., Gao, H., Li, M., Chen, Z., 2021. Design and optimization of the direct recycling of spent Li-ion battery cathode materials. ACS Sustain. Chem. Eng. 9, 4543-4553. https://doi.org/10.1021/acssuschemeng.0c09017.

Wu, W., Liu, X., Zhang, X., Zhu, M., Tan, W., 2018. Bioleaching of copper from waste printed circuit boards by bacteria-free cultural supernatant of iron–sulphur-oxidizing bacteria. Bioresour. Bioprocess. 5, 1-13. https://doi.org/10.1186/s40643-018-0196-6.

Yang, Y., Chen, S., Li, S., Chen, M., Chen, H., and Liu, B.: Bioleaching waste printed circuit boards by *Acidithiobacillus ferrooxidans* and its kinetics aspect, J. Biotechnol. 173, 24e30 (2014). https://doi.org/10.1016/j.jbiotec.2014.01.008.

You, J., Solongo, S. K., Gomez-Flores, A., Choi, S., Zhao, H., Urik, M., Kim, H., 2020. Intensified bioleaching of chalcopyrite concentrate using adapted mesophilic culture in continuous stirred tank reactors. Bioresour. Technol. 307, 123181. https://doi.org/10.1016/j.biortech.2020.123181.

Zhang, L., Zhou, W., Liu, Y., Jia, H., Zhou, J., Wei, P., Zhou, H., 2020. Bioleaching of dewatered electroplating sludge for the extraction of base metals using an adapted microbial consortium: Process optimization and kinetics. Hydrometallurgy. 191, 105227. https://doi.org/10.1016/j.hydromet.2019.105227.

Fig. 1. Schematic diagram of the whole process for Cu recovery.

Fig. 2. Bio-oxidation of iron in the continuous culture of *A. ferrooxidans* in STR.

Fig. 3. Effect of (a) pulp density in a batch leaching in a flask scale and (b) pH variation during the batch leaching in a flask scale.

Fig. 4. (a) Effect of pH adjustment on the leaching rate of Cu and (b) pH and Eh variations in samples with and without pH adjustment. (pH 1: with pH adjustment, pH 2: without pH adjustment, Eh 1: with pH adjustment and Eh 2: without pH adjustment).

Fig. 5. Effect of (a) temperature and (b) HRT on Cu leaching.

Fig. 6. Pourbaix diagram for (a) Fe-SO_4 system and (b) Fe-Cu system when Cu^{2+} is the predominant species and (c) Fe-Cu system when Fe is the predominant species at 25 °C simulated by Hydra-Medusa software (total Fe = 180 mM, SO_4^{2-} = 4.5 mM, Cu^{2+} = 132 mM).

Fig. 7. XRD analyses of (a) pre-leached powder, (b) after the batch leaching in a flask and (c) after the continuous leaching in STR.

Fig. 8. FE-SEM analysis of (a) pre-leached powder, (b) after the batch leaching, (c) after the continuous leaching in STR and mapping under three different conditions.

Fig. 9. (a) Mass of Cu deposited on cathode surface (practical versus theoretical) and current efficiency over time, (b) Cathode surface during the electrowinning process before electrowinning, (c) after 4 h, (d) after 8 h, (e) Cu foil with 86.76% purity and (f) EDX analysis of Cu foil after the electrowinning process.

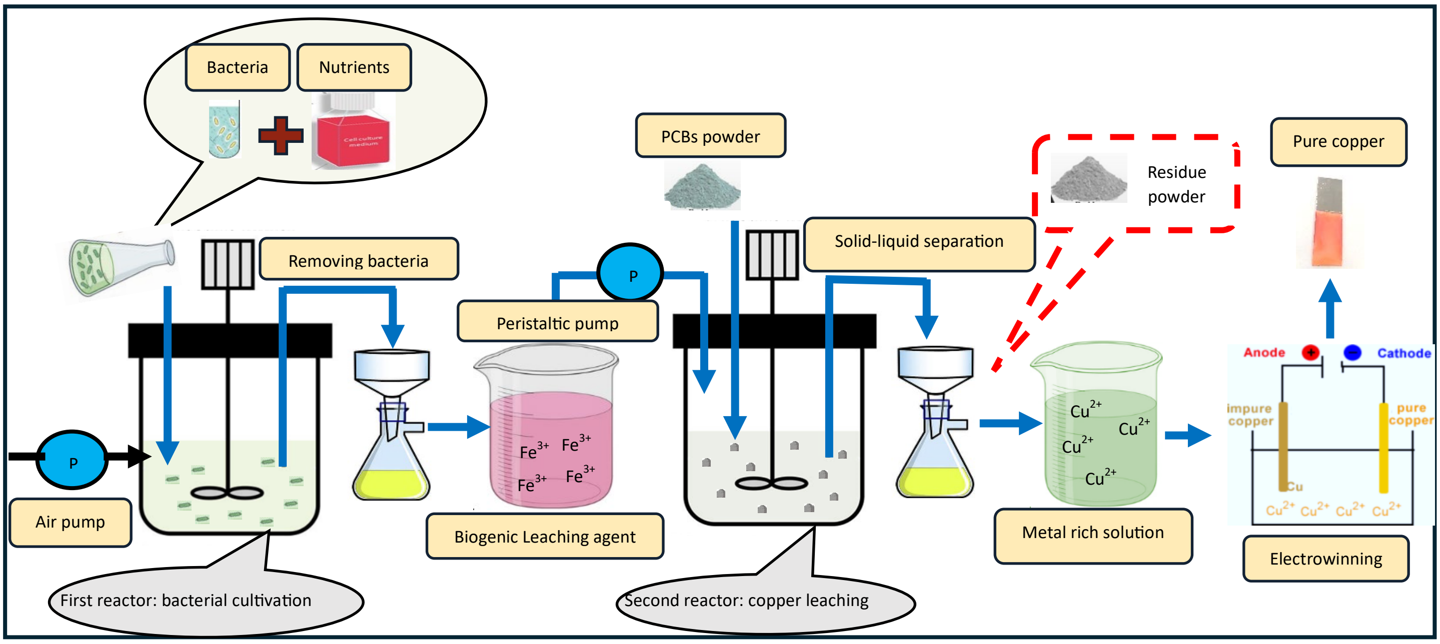
Bacteria
Nutrients
Removing bacteria
Air pump
P
First reactor: bacterial cultivation
Peristaltic pump
P
Fe^{3+} Fe^{3+} Fe^{3+} Fe^{3+}
Biogenic Leaching agent
PCBs powder
Solid-liquid separation
Second reactor: copper leaching
Residue powder
Cu^{2+} Cu^{2+} Cu^{2+} Cu^{2+}
Metal rich solution
Pure copper
Anode
Cathode
impure copper
pure copper
Cu
Cu^{2+} Cu^{2+} Cu^{2+} Cu^{2+}
Electrowinning

Fig. 1.

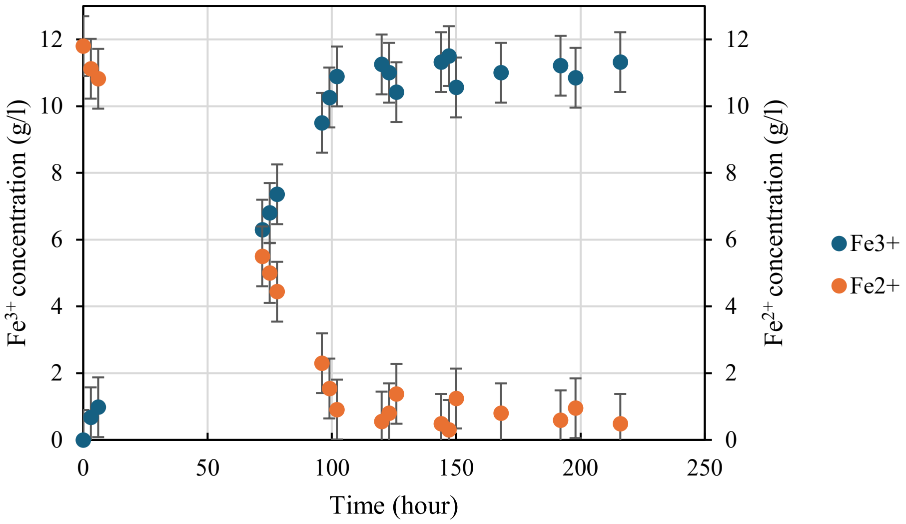
Fe^{3+} concentration (g/l)
Fe^{2+} concentration (g/l)
0
2
4
6
8
10
12
0
50
100
150
200
250
Time (hour)
● Fe3+
● Fe2+

Fig. 2.

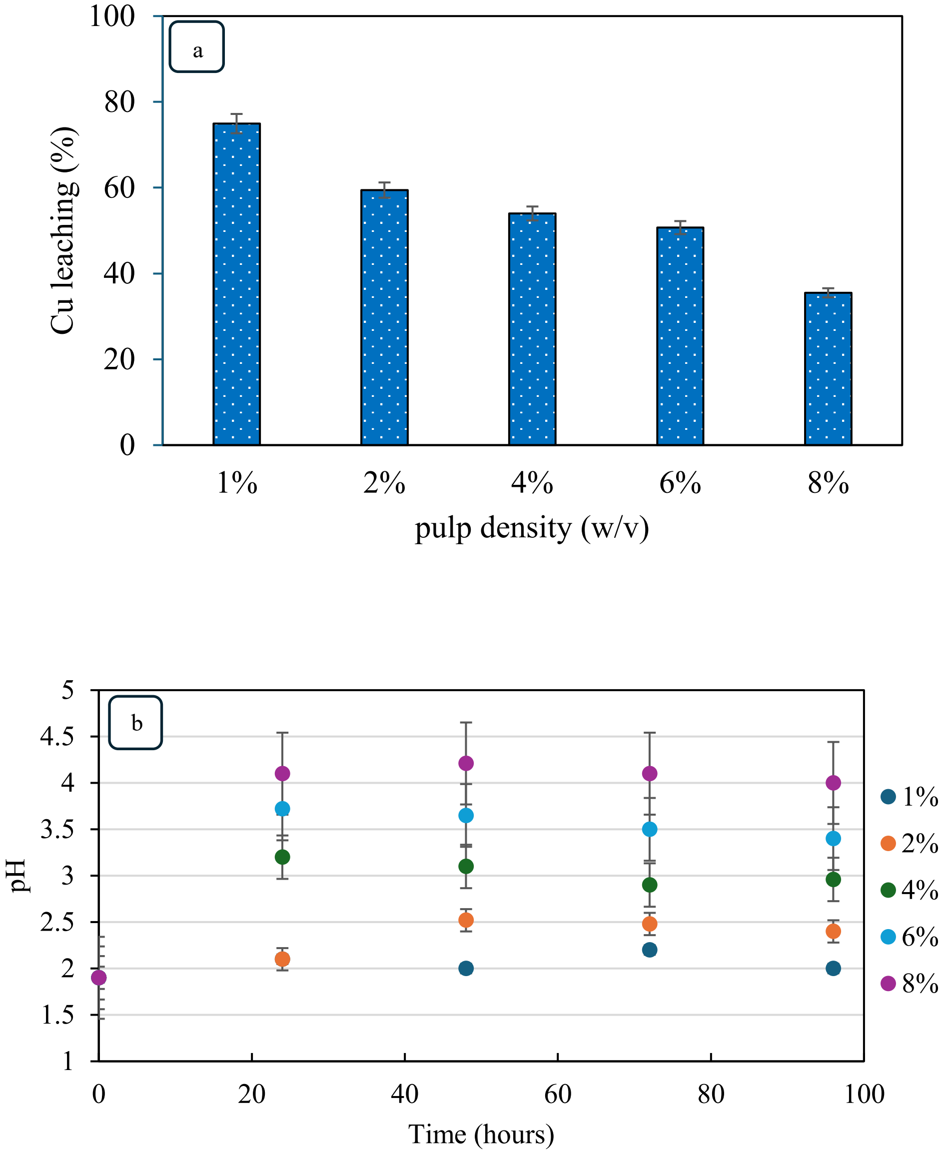
a
Cu leaching (%)
100
80
60
40
20
0
1%
2%
4%
6%
8%
pulp density (w/v)
b
pH
5
4.5
4
3.5
3
2.5
2
1.5
1
0
20
40
60
80
100
Time (hours)
● 1%
● 2%
● 4%
● 6%
● 8%

Fig. 3.

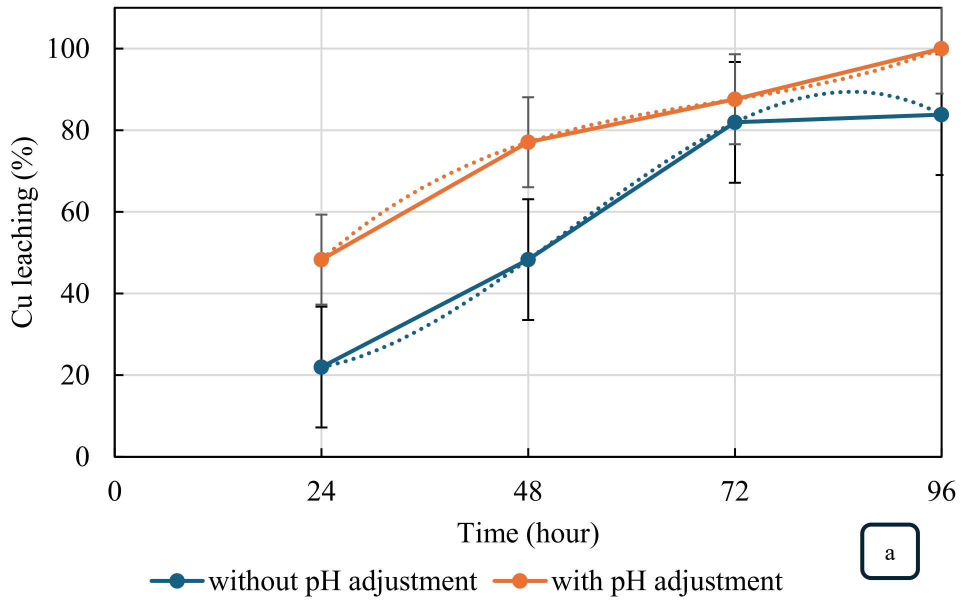
Cu leaching (%)
0
20
40
60
80
100
0
24
48
72
96
Time (hour)
a
without pH adjustment
with pH adjustment

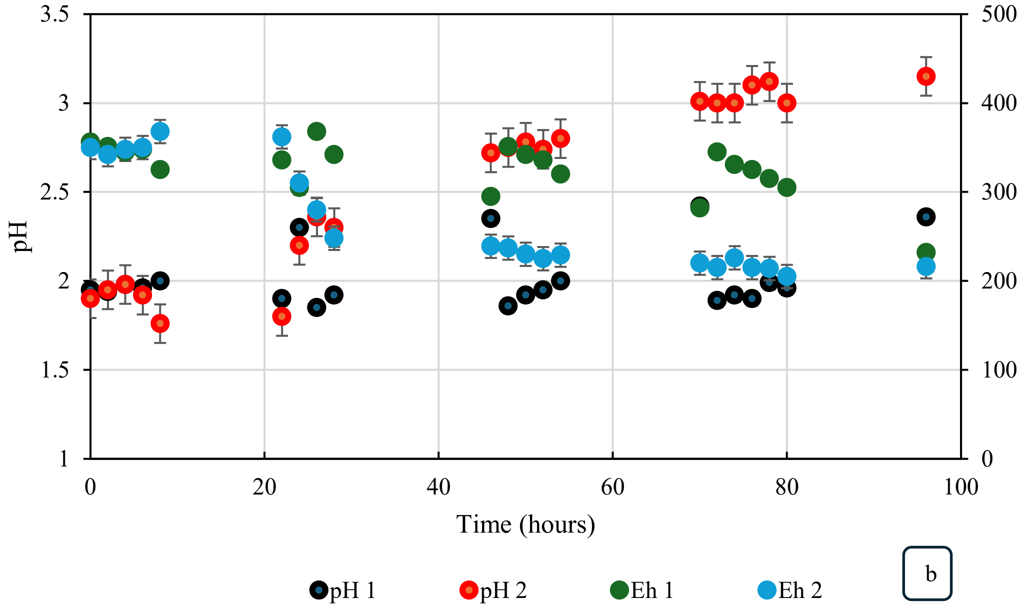
pH
3.5
3
2.5
2
1.5
1
500
400
300
200
100
0
0
20
40
60
80
100
Time (hours)
b
pH 1
pH 2
Eh 1
Eh 2

Fig. 4.

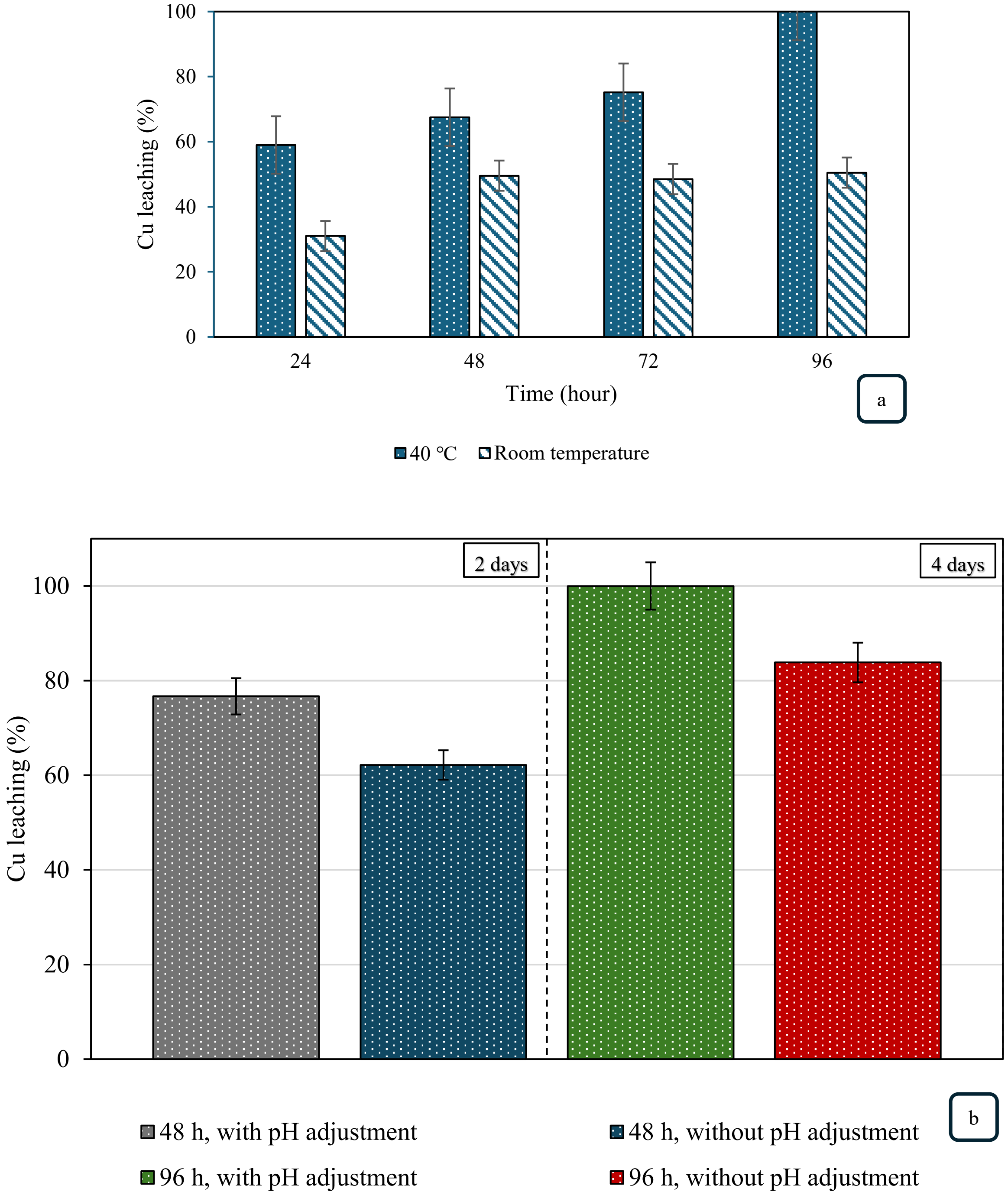
100
80
60
40
20
0
Cu leaching (%)
24
48
72
96
Time (hour)
a
40 °C
Room temperature
2 days
4 days
100
80
60
40
20
0
Cu leaching (%)
b
48 h, with pH adjustment
48 h, without pH adjustment
96 h, with pH adjustment
96 h, without pH adjustment

Fig. 5.

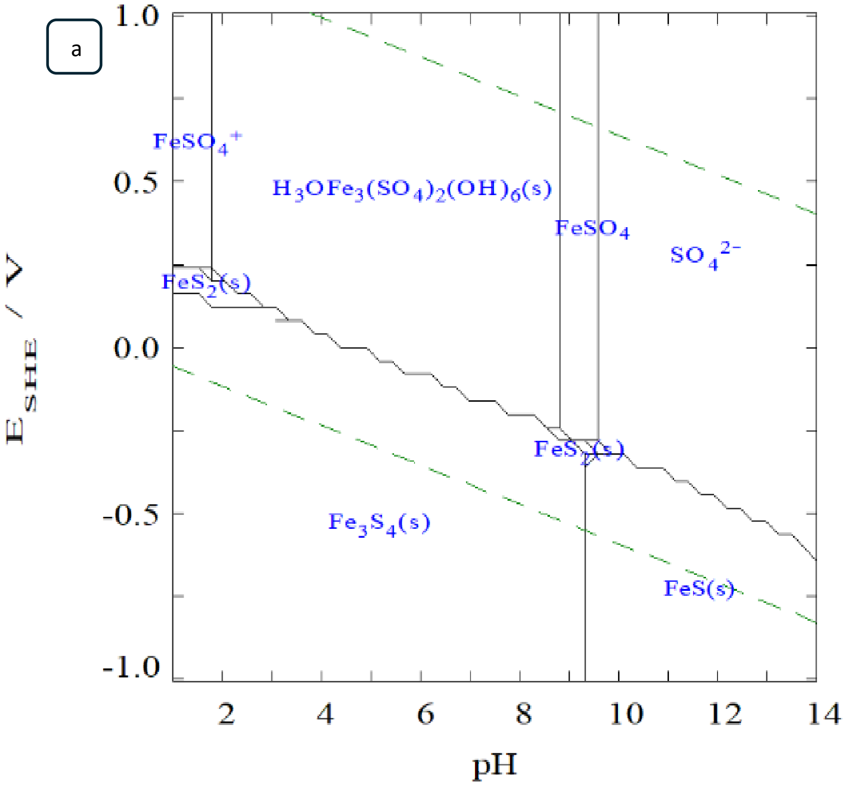
a
1.0
0.5
0.0
-0.5
-1.0
E_{SHE} / V
$FeSO_4^+$
$H_3OFe_3(SO_4)_2(OH)_6(s)$
$FeSO_4$
SO_4^{2-}
$FeS_2(s)$
$FeS_2(s)$
$Fe_3S_4(s)$
FeS(s)
2
4
6
8
10
12
14
pH

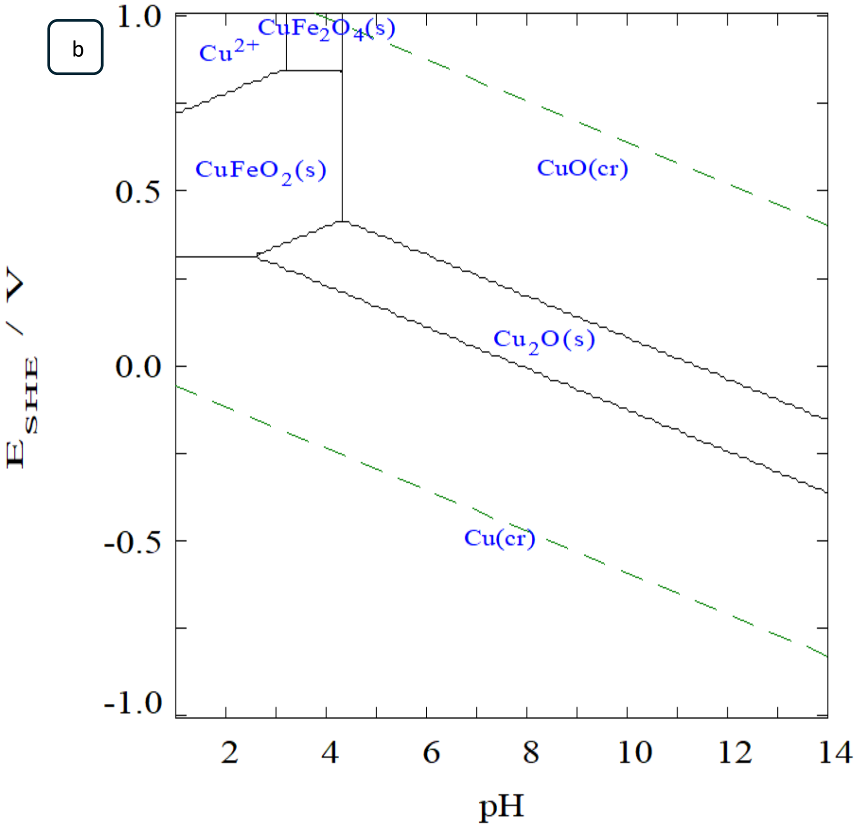
b
1.0
0.5
0.0
-0.5
-1.0
E_{SHE} / V
Cu^{2+}
$CuFe_2O_4(s)$
$CuFeO_2(s)$
CuO(cr)
$Cu_2O(s)$
Cu(cr)
2
4
6
8
10
12
14
pH

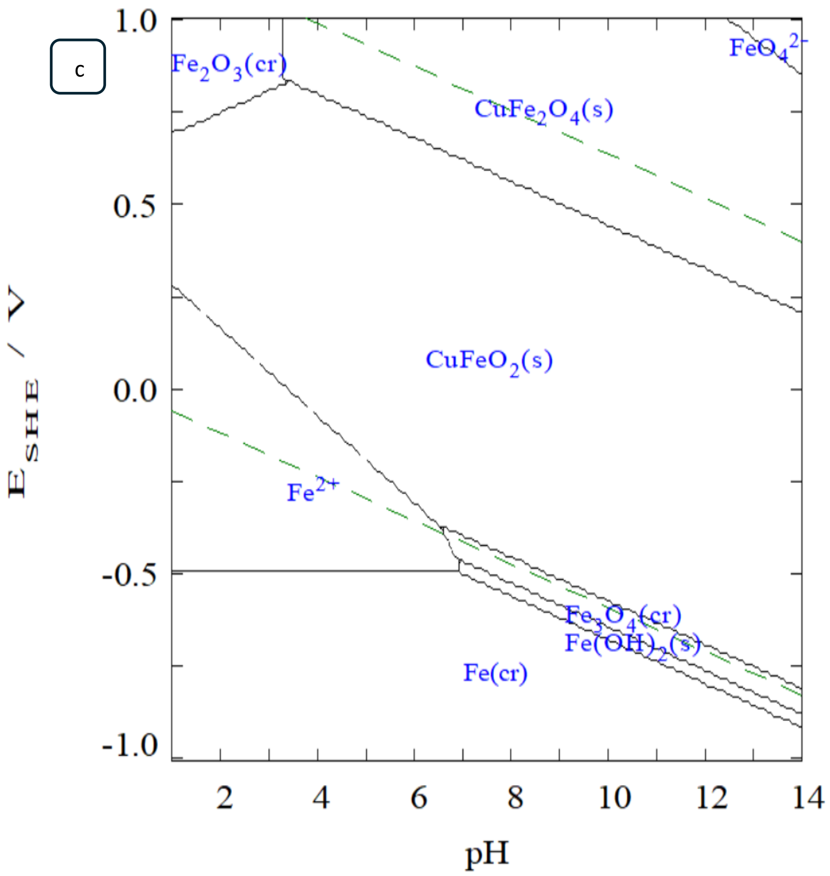
c
1.0
0.5
0.0
-0.5
-1.0
E_{SHE} / V
2
4
6
8
10
12
14
pH
$Fe_2O_3(cr)$
FeO_4^{2-}
$CuFe_2O_4(s)$
$CuFeO_2(s)$
Fe^{2+}
$Fe_3O_4(cr)$
$Fe(OH)_2(s)$
Fe(cr)

Fig. 6.

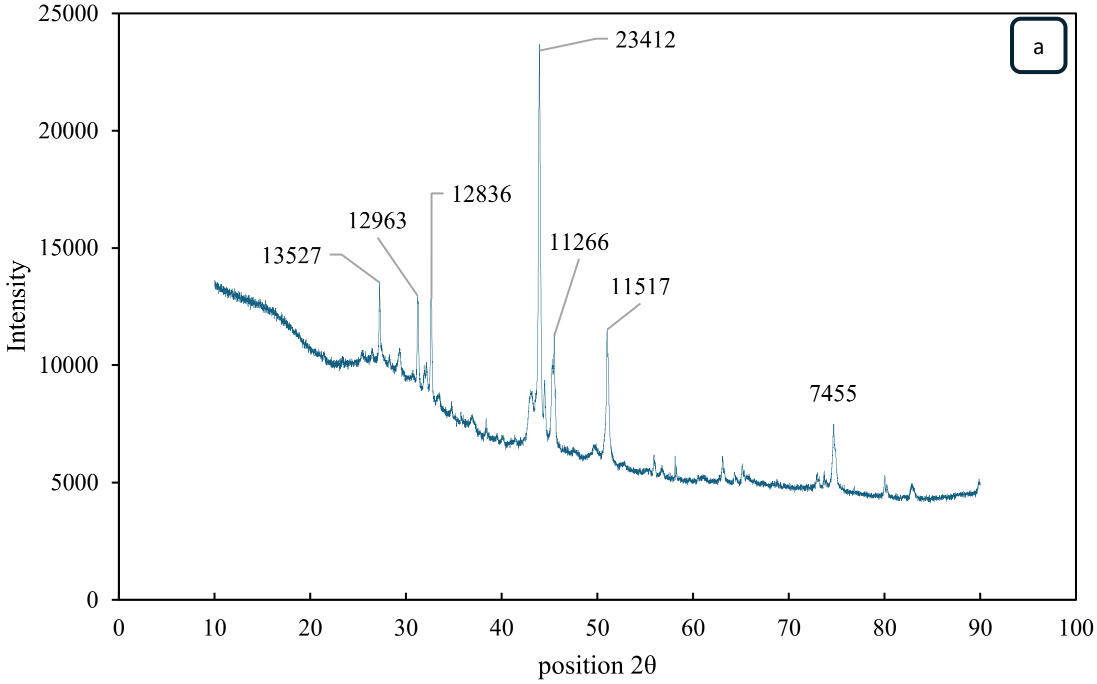
a
25000
20000
15000
10000
5000
0
Intensity
0
10
20
30
40
50
60
70
80
90
100
position 2θ
23412
12836
12963
13527
11266
11517
7455

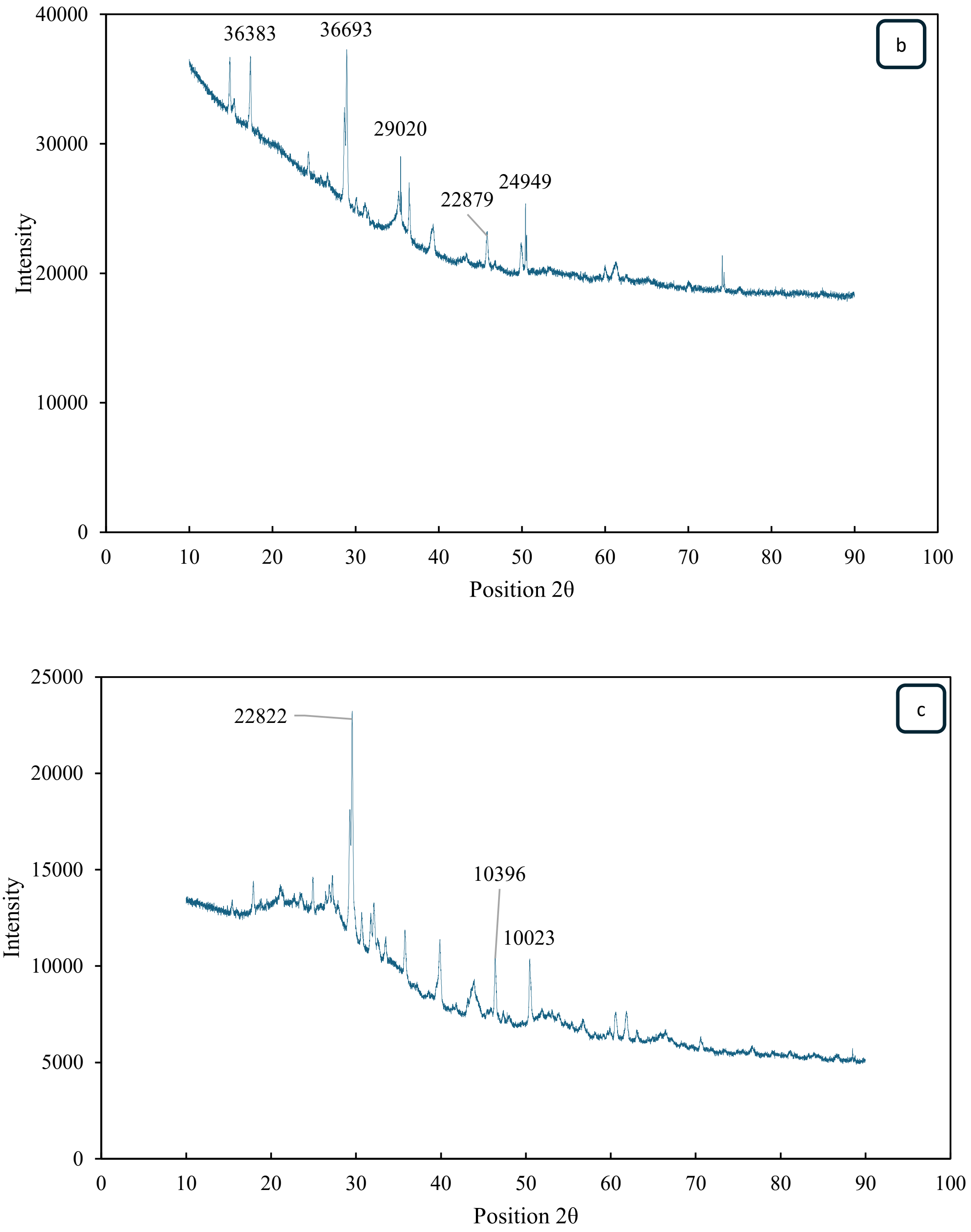
b
Intensity
Position 2θ
36383
36693
29020
22879
24949
0
10000
20000
30000
40000
0
10
20
30
40
50
60
70
80
90
100
c
Intensity
Position 2θ
22822
10396
10023
0
5000
10000
15000
20000
25000
0
10
20
30
40
50
60
70
80
90
100

Fig. 7.

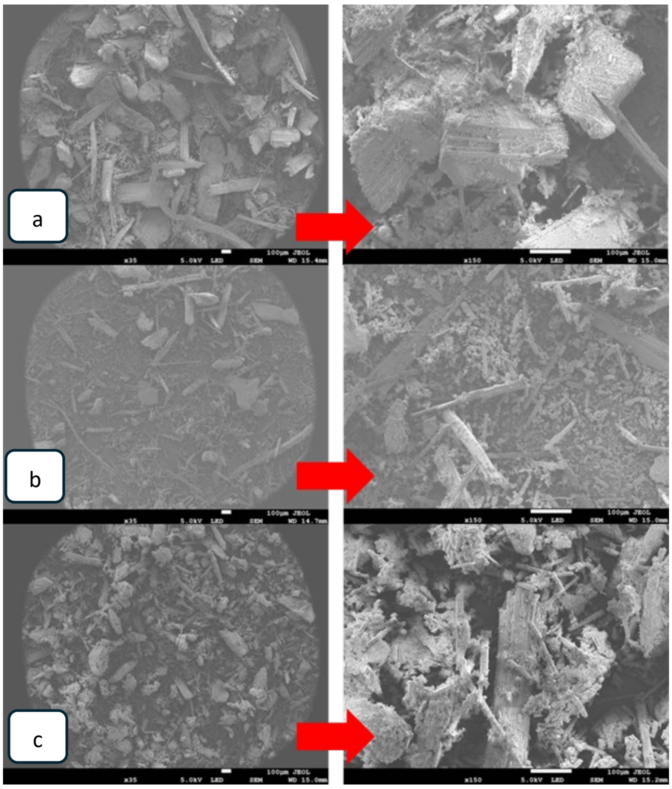
a
100µm JEOL
x35 5.0kV LED SEM WD 15.4mm
100µm JEOL
x150 5.0kV LED SEM WD 15.0mm
b
100µm JEOL
x35 5.0kV LED SEM WD 14.7mm
100µm JEOL
x150 5.0kV LED SEM WD 15.0mm
c
100µm JEOL
x35 5.0kV LED SEM WD 15.0mm
100µm JEOL
x150 5.0kV LED SEM WD 15.2mm

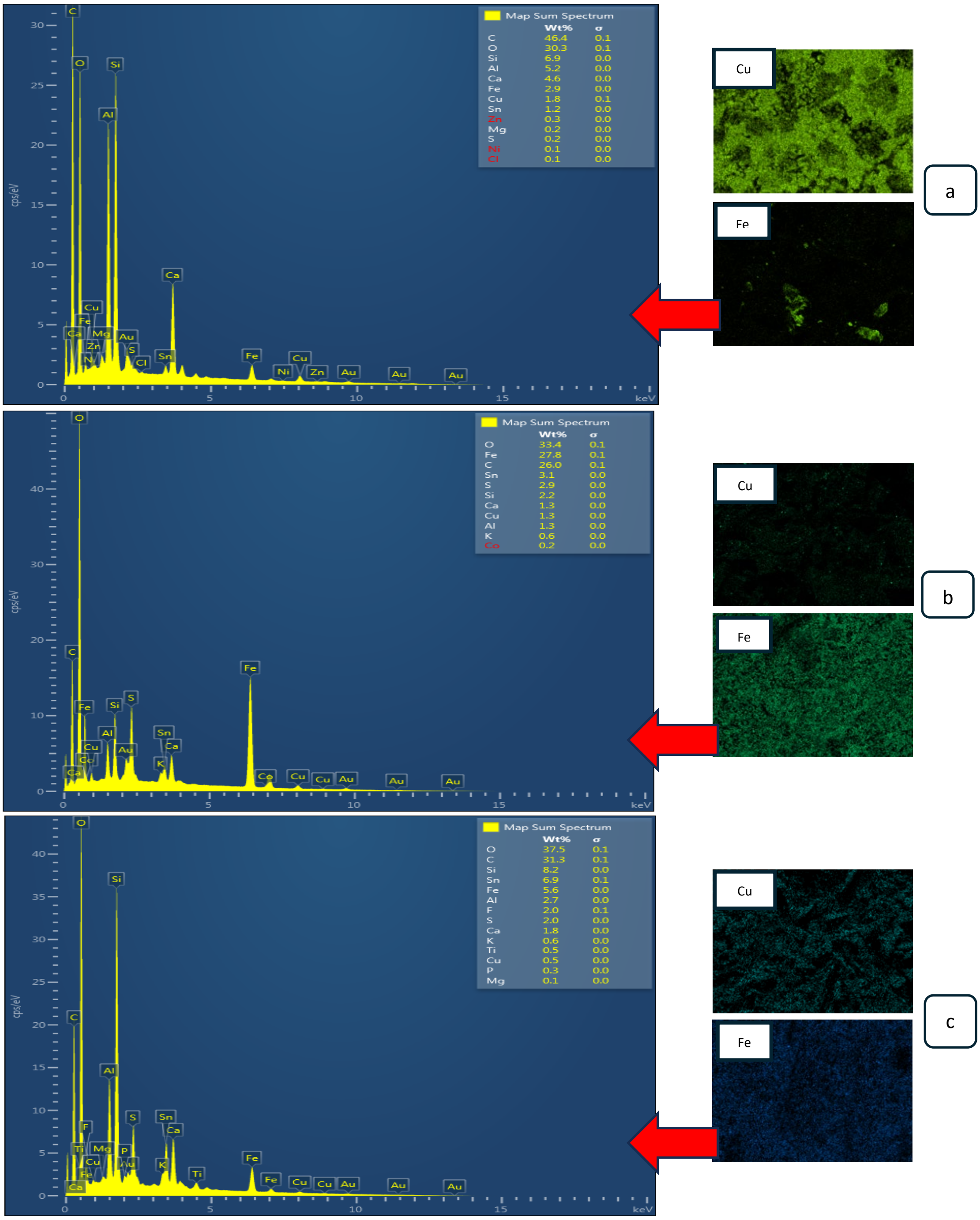

Map Sum Spectrum

	Wt%	σ
C	46.4	0.1
O	30.3	0.1
Si	6.9	0.0
Al	5.2	0.0
Ca	4.6	0.0
Fe	2.9	0.0
Cu	1.8	0.1
Sn	1.2	0.0
Zn	0.3	0.0
Mg	0.2	0.0
S	0.2	0.0
Ni	0.1	0.0
Cl	0.1	0.0

Map Sum Spectrum

	Wt%	σ
O	33.4	0.1
Fe	27.8	0.1
C	26.0	0.1
Sn	3.1	0.0
S	2.9	0.0
Si	2.2	0.0
Ca	1.3	0.0
Cu	1.3	0.0
Al	1.3	0.0
K	0.6	0.0
Co	0.2	0.0

Map Sum Spectrum

	Wt%	σ
O	37.5	0.1
C	31.3	0.1
Si	8.2	0.0
Sn	6.9	0.1
Fe	5.6	0.0
Al	2.7	0.0
F	2.0	0.1
S	2.0	0.0
Ca	1.8	0.0
K	0.6	0.0
Ti	0.5	0.0
Cu	0.5	0.0
P	0.3	0.0
Mg	0.1	0.0

Fig. 8.

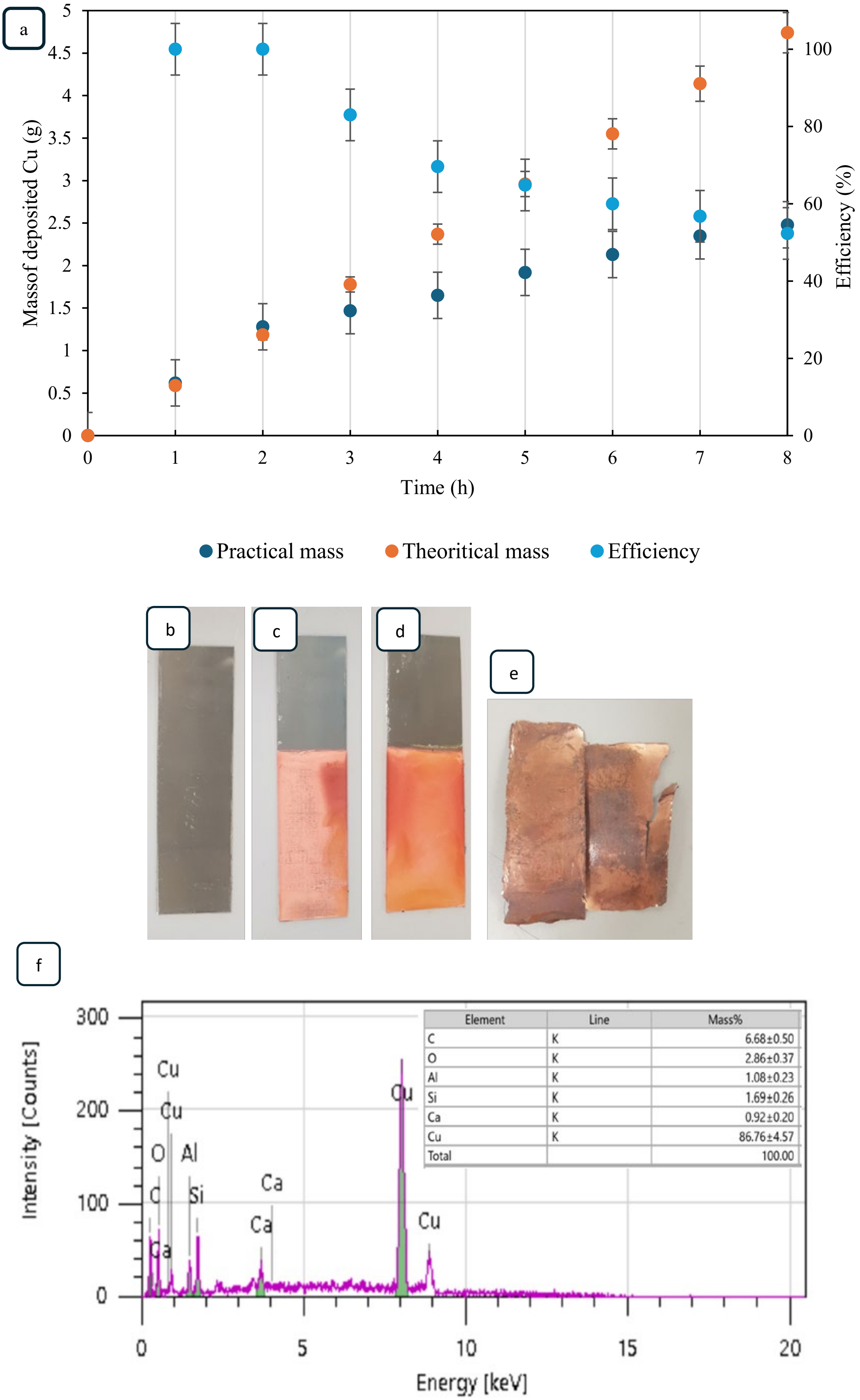

Element	Line	Mass%
C	K	6.68±0.50
O	K	2.86±0.37
Al	K	1.08±0.23
Si	K	1.69±0.26
Ca	K	0.92±0.20
Cu	K	86.76±4.57
Total		100.00

Fig. 9

Table 1. Elemental composition of waste PCB (mg/g $_{\text{powder}}$).

Table 2 Continuous iron oxidation rate by acidophilic bacteria in different studies.

Table 3 Examples of bioleaching studies conducted at high pulp densities.

Table 4 Dissolution rate (mg/ l d) of Cu under different conditions (with pH adjustment and without pH adjustment).

Table 5. Cu concentration in the metal rich solution after the leaching.

Table 6. Metal concentrations in the post leaching solution.

Table 1.

Element	Cu	Al	Fe	Mn	Mg	Ni	Au	Pb
Concentration (mg/g)	193.06	28.57	49.98	0.11	1.51	2.93	0.074	5.27

Table 2.

Highest Fe^{2+} concentration (g/l)	HRT (h)	Bio-oxidation rate (mg/l h)	References
8.5	16 to 100	450	(Gó Mez and Cantero, 2003)
15	6 to 45	1100	(Kaksonen et al., 2014b)
12	10 to 66	950	(Ojumu and Petersen, 2011)
9	6.3	1400	(Hubau et al., 2018)
7	24 to 96	469	Present work

Table 3.

Microorganism	**Pulp density (%w/v)**	**Extraction (%)**	**Conditions**	**Waste**	**References**
A. ferrooxidans and *A. thiooxidans*	10	Cu: 94 Ni: 89 Zn: 88 Al: 59	30 °C, 180 rpm, 10 d	PCBs	(Arslan, 2021)
A. thiooxidans and *L. ferriphilum*	8	Zn: 29.9 Mn: 2.5	35 °C, 120 rpm, 13 d	Zn-Mn battery	(Xin et al., 2012)
S. thermosulfdooxidans and *T. acidophilum*	10	Zn: 74 Al: 68 Cu: 85 Ni: 78	45 °C, pH 2, 165 d	Electronic scrap	(Ilyas et al., 2013)
A. ferrooxidans	3.5	Cu: 92	pH 1.8, 30 °C, 170 rpm	Computer PCBs	(Shin et al., 2013)
A. *ferrooxidans, L. ferrooxidans* and *A. thiooxidans*	7 15	Ni: 20.39 Ni: 47.9	30 °C, 150 rpm, 8 d	Waste PCBs	(Erust et al., 2020)
Thermophilic consortium	10	Cu: 64	45 °C, 450 and 200 rpm, 6 d	Low-grade chalcopyrite	(Gericke et al., 2010)
sulphur- and iron-oxidizing bacteria	10	Heavy REE: 58 Light REE: 14 Th: 89	30°C, 900 rpm, 35 d	Uranium tailing	(Reynier et al., 2021)
A. ferrooxidans	6	Cu: 50.7	40 °C, 200 rpm, 4 d	PCBs	Present work

Table 4.

Status	Dissolution rate of Cu (mg/ l d)
With pH adjustment	

First day	4,200
Second day	5,500
Third day	2,660
Fourth day	1,750
Without pH adjustment	
First day	2,480
Second day	2,210
Third day	3,660
Fourth day	2,650

Table 5.

Condition	Cu concentration after the leaching (mg/l)
Room temperature, with pH adjustment, 96 h	5,850
40 °C, with pH adjustment, 96 h	12,550
40 °C, without pH adjustment, 96 h	11,000
40 °C, with pH adjustment, 48 h	8,880
40 °C, without pH adjustment, 48 h	7,200

Table 6.

Metal	Concentration (mg/l)	Leaching rate (%)
Cu	11,000	94.96
Mg	72	79.41
Ni	40	22.75
Al	3.55	0.2